GCAGS JOURNAL A Publication of the Gulf Coast Association of Geological Societies
www.gcags.org

Depositional Systems, Facies Variability, and Reservoir Quality in Shallow-Marine Reservoirs in the Eocene Upper Wilcox Group in Fandango Field, Zapata County, Texas

William A. Ambrose, Shirley P. Dutton, and Robert G. Loucks

Bureau of Economic Geology, Jackson School of Geosciences, University of Texas at Austin, University Station, Box X, Austin, Texas 78713–8924, U.S.A.

ABSTRACT

Deeply-buried (>13,000 ft [>3960 m]) reservoirs of shallow-marine origin in the Eocene upper Wilcox Group in Fandango Field in Zapata County, Texas have low-permeability and moderate-to-low porosity values (commonly <1 md and <15%, respectively). From a dataset of 7 whole cores that collectively compose ~1070 ft (~326 m) of section within a depth range from 13,725 to 18,183 ft (4184 to 5544 m), this study interprets a wave-dominated, microtidal (diurnal tidal range <6.6 ft [<2 m]) setting for the upper Wilcox Group in Fandango Field. Upper-shoreface and proximal-delta-front facies in Fandango Field are upward coarsening and feature multiple, scour-based beds of planar-stratified, upper-fine-grained sandstone and burrowed beds with *Ophiomorpha* and lesser *Planolites*. In contrast, lower- and middle-shoreface facies are extensively burrowed, featuring *Palaeophycus*, *Schaubcylindrichnus*, and *Asterosoma* with subordinate *Ophiomorpha*. Modern depositional analogs for the upper Wilcox Group in Fandango Field include the wave-dominated Santee Delta and Cape Romain in South Carolina, whereas upper-shoreface and wave-dominated deltaic deposits in the Upper Cretaceous (Campanian) Pictured Cliffs Sandstone in the San Juan Basin in New Mexico and Colorado serve as an ancient facies analog.

Crossplots of grain size versus porosity and permeability in the upper Wilcox succession in Fandango Field from a dataset of 347 plugs from whole cores indicate that grain size and facies origin are poor predictors of reservoir quality, defined as porosity and permeability. However, some facies display variation in reservoir quality, expressed in terms of range and average values of porosity and permeability. Optimal reservoir quality occurs in sandy upper-shoreface/proximal-delta-front facies and transgressive deposits. Relatively high values of average porosity (14.2 to 16.5%) occur in amalgamated, fine-grained sandstone beds in upper-shoreface/proximal-delta-front facies, whereas lower values (<9%) are prevalent in lower-shoreface/distal-delta-front facies. Similarly, greater values of permeability occur within upper-shoreface/proximal-delta-front and transgressive deposits, with average values of 3.56 and 2.80 md in upper-shoreface/proximal-delta-front and transgressive deposits, respectively. In contrast, average permeability values are much lower (0.14 md) in lower-shoreface/distal-delta-front facies.

This study concludes that grain size and facies variability in the upper Wilcox succession in Fandango Field are poor indicators of reservoir quality. Other factors such as diagenesis may control reservoir quality and should also be considered in reservoir development in Fandango Field and other fields in the South Texas Wilcox trend.

INTRODUCTION

During early Eocene time (50 Ma), the area of Fandango Field, located in Zapata County in South Texas (Fig. 1), occupied a coastal position in a transitional area between wave-dominated deltaic and shoreface depositional systems (Galloway et al., 2000; Blakey, 2014). The upper Wilcox Group in Fandango Field was deposited along a major depositional axis associated with the ancestral Rio Grande Delta. Major sediment sources are inferred from the Mogollon Highlands in southern Arizona and southwestern New Mexico (Galloway et al., 2011).

Low-permeability (commonly <1 md) gas reservoirs in Fandango Field are trapped within a faulted anticline developed on the downthrown side of a major growth fault associated with the late Wilcox shelf edge (Fig. 2). (Hargis, 1985; Robinson et al., 1986; Stricklin, 1994; Debus, 1996; Meyerhoff and Braddock, 1998). Low-permeability gas reservoirs in the upper Wilcox section in Fandango Field commonly require hydraulic fracturing to stimulate production. Sandstone bodies in the field are overpressured and produce gas at high rates of 3000 to 5000 Mcf/d

Manuscript received March 17, 2016; revised manuscript received June 24, 2016; manuscript accepted July 13, 2016.

GCAGS Journal, v. 5 (2016), p. 73–94.

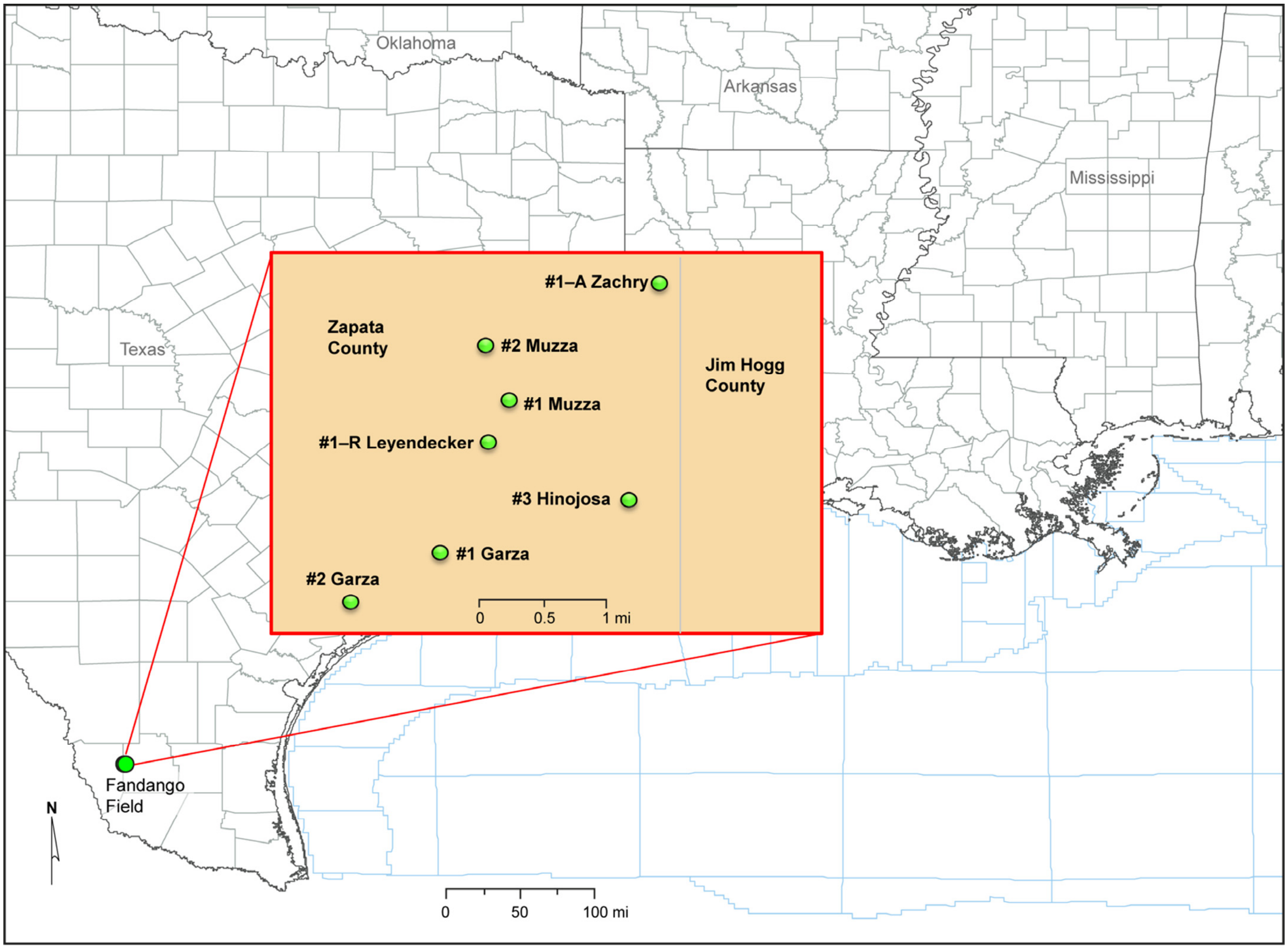

Figure 1. Location of Fandango Field in Zapata County, Texas, and distribution of Upper Wilcox cores in this study. Structure map of Fandango Field and distribution of cores are shown in Figure 2.

(thousand cubic ft per day). Bottomhole pressures commonly exceed 12,000 psi, with elevated bottomhole temperatures >400°F (>205°C) (Levin, 1983).

Reservoirs in Fandango Field occur within predominantly upward-coarsening shallow-marine parasequences that individually range from 100 to 250 ft (30.5 to 76.2 m) thick (Fig. 2). These shallow-marine parasequences represent a variety of shoreface, beach, and inner-shelf facies as well as wave-dominated deltaic environments that include delta-front, channel-mouth-bar, and distributary-channel facies (Joyce, 1954; Rolf, 1987; Levin, 1983). The diurnal tidal regime for these upper Wilcox shallow-marine parasequences is interpreted to be microtidal, defined as a diurnal tidal range <6.6 ft (<2 m) (Davies, 1964). This interpretation is based on great strike-continuity of main framework sandstone bodies (Levin, 1993; Meyerhoff and Braddock, 1998), consistent with a wave-dominated coastal setting and barrier-island morphology along microtidal shorelines (Hoyt and Henry, 1967; Hayes, 1976, 1979; Wilkinson and Basse, 1978; Galloway and Cheng, 1985; Galloway, 1986). Debus (1996) and Meyerhoff and Braddock (1998) document extreme strike-elongate (southwest-to-northeast) sandstone-body continuity (>30 mi [>48 km]) in upper Wilcox reservoirs, also consistent with a wave-dominated shoreline setting. A microtidal regime for the upper Wilcox section in Fandango Field is also consistent with the absence of features such as rhythmic stratification, lenticular beds, flaser ripples, and double-draped ripples in cores in the field, features that are common in tidally modified or tide-dominated settings (Reineck and Wunderlich, 1968; de Mowbray and Visser, 1984; Kvale et al., 1989; Kvale and Archer, 1990; White et al., 2004; Dalrymple and Choi, 2007).

OBJECTIVES, DATA, AND METHODS

The three objectives of this study are to: (1) provide a set of descriptions of cores in the upper Wilcox Group in Fandango Field; (2) interpret sedimentary processes and depositional facies from core and wireline logs of these cored wells; and (3) describe relationships between grain size and reservoir quality (porosity and permeability) for individual facies, as well as for combined facies.

Whole cores from the upper Wilcox Group in Fandango Field illustrate a variety of systems tracts, depositional systems and facies, and provide a context for reservoir-quality data. This study summarizes porosity and permeability data, as well as selected descriptions and facies interpretation from a set of whole cores from 7 wells (located in Figure 2) from Fandango Field that collectively comprise ~1070 ft (~326 m) of section from the upper Wilcox Group. Core descriptions from 5 of these 7 wells are included in this report to reduce redundancy in facies descriptions. Data recorded in these whole core descriptions include grain size, stratification, contacts, as well as accessory features such as soft-sediment deformation, burrows, clay clasts, roots,

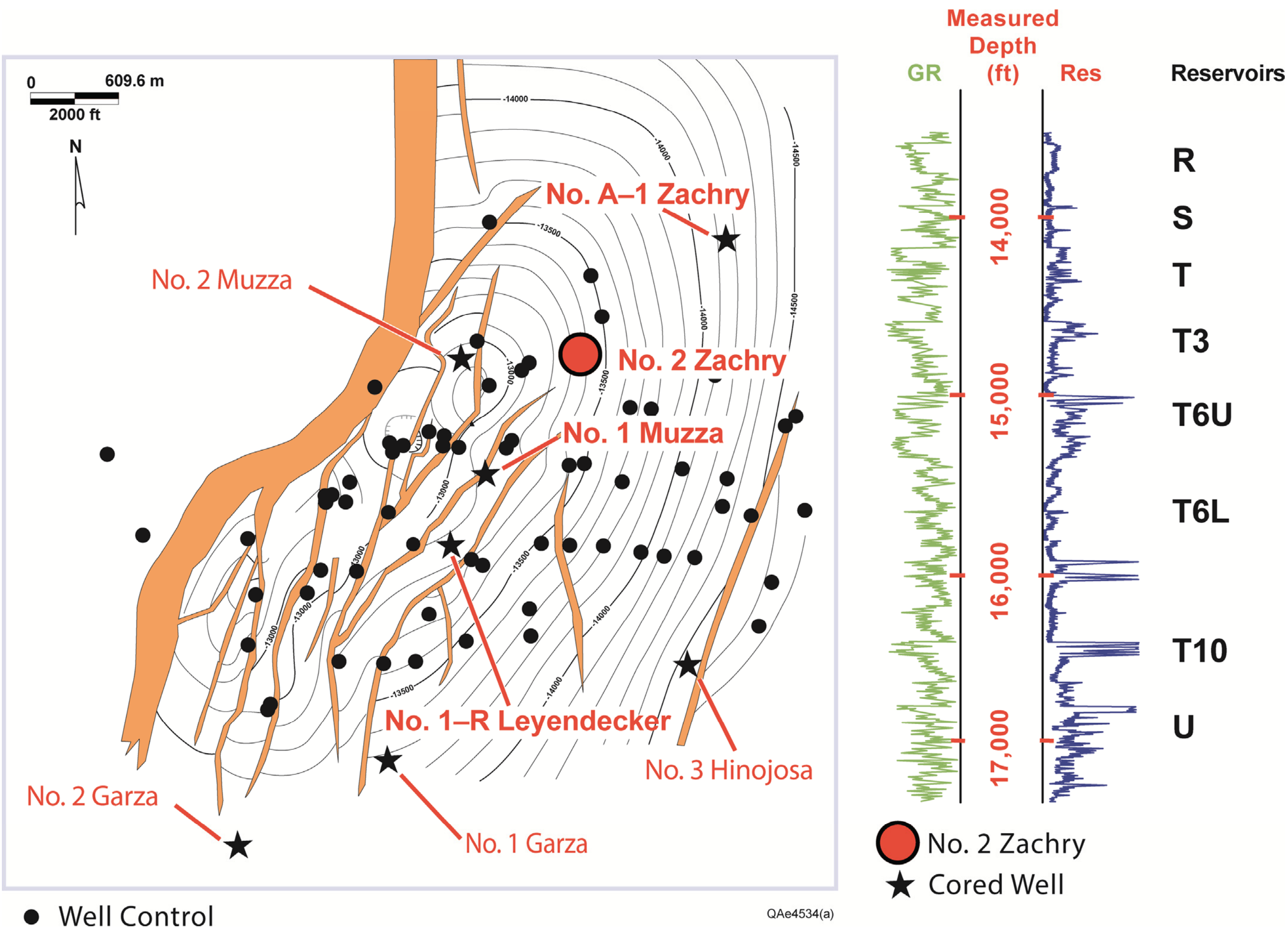

Figure 2. Structure map and type log, Fandango Field. Distribution of wells with cores in this study also shown. Regional location of Fandango Field is shown in Figure 1. Courtesy of Comstock Resources, Inc.

and shell and organic fragments that are diagnostic of sedimentary processes and depositional environments. These core descriptions are also supplemented by photographs that illustrate facies, and reservoir quality. Depositional systems and facies interpretations are made by integrating core descriptions, accessory features, and wireline-log responses of cored wells.

A structure map of Fandango Field, illustrating distribution of wells and production data from cored wells, provided by Comstock Resources, Inc., was integrated into the study. Other data integrated with core descriptions and facies interpretations include porosity and permeability data from plugs. A total of 347 data points for porosity and 286 data points for permeability from plugs from the full set of 7 whole cores are used to document relationships between grain size (expressed in terms of ϕ units) and porosity and permeability values for all combined depositional systems and facies, as well as individual facies in the upper Wilcox succession in Fandango Field.

Two primary depositional systems in the upper Wilcox Group in Fandango Field, recognized from cores in this study, are summarized in Table 1—distal-shoreline and proximal-shoreline. Distal-shoreline systems in Fandango Field include lower shoreface/distal-delta-front and middle shoreface/medial-delta-front facies, whereas proximal-shoreline systems include upper-shoreface/proximal-delta-front and transgressive deposits. Recognition criteria for each facies are summarized in Table 1. Reservoir-quality data (porosity and permeability) for each facies, presented in Tables 2 and 3, are described in the section "Controls on Porosity and Permeability" in this report.

Other geologic controls on reservoir quality in the upper Wilcox succession in South Texas include compaction, variations in mineralogy, and temperature (Loucks et al., 1984, 1986; Dutton, 1987; Dutton and Loucks, 2010; Taylor et al., 2010). A companion paper (Dutton et al., 2016, this volume) documents these factors as they are related to reservoir quality in Fandango Field. The goal of this paper, however, is to describe any relationships between grain size versus porosity and permeability that may exist for the upper Wilcox succession, and not to examine later diagenetic modifications to reservoir quality.

DISTAL-SHORELINE SYSTEMS

Distal-shoreline systems in upper Wilcox cores in Fandango Field, which include distal-delta-front and lower- to middle-shoreface facies, are characterized by thick (commonly >50 ft [>15 m]) sections of silty mudstone interbedded with thin (<4 in [<10.2 cm]) beds of very fine-grained sandstone. Recognition criteria for distal-shoreline systems, discussed in this section, are applied to the Shell No. 1–R Leyendecker and Shell No. 1 Muzza cores, located in Figure 2.

Analogs with similar distal-deltaic and lower-shoreface facies include the Olmos Formation in the Maverick Basin (Tyler and Ambrose, 1986), the middle Miocene in Galveston County (Ambrose, 1990), the Woodbine Group in southeast Texas (Ambrose and Hentz, 2012), and the San Juan Basin in New Mexico and Colorado (Flores and Erpenbeck, 1979; Cumella, 1981; Condon et al., 1997; Ambrose and Ayers, 2007). Stratifi-

Table 1. Principal depositional facies in cores in the Upper Wilcox section in Fandango Field, together with recognition criteria for each facies.

Depositional Systems	Facies	Recognition Criteria	Figures
Distal-shoreline	Lower shoreface/distal-distal-front	Thin sandstones within sparsely burrowed and upward-coarsening, muddy intervals	3, 4, and 11B
Distal-shoreline	Middle shoreface/medial-delta-front	Burrowed, upward-coarsening intervals with *Planolites* and *Palaeophycus* predominant	5 and 6
Proximal-shoreline	Upper-shoreface/proximal-delta-front	Planar-stratified and burrowed, upward-coarsening intervals with *Ophiomorpha* predominant	7, 8, 10, 11A, and 11C
Proximal-shoreline	Transgressive deposits	Erosion-based, upward-fining sections at top of upward-coarsening successions	10

Table 2. Summary of porosity data for each principal depositional facies listed in Table 1.

Depositional Systems	Facies (n)	Depth Range (ft)	Porosity Range (%)	Average Porosity (%)
Distal-shoreline	Lower shoreface/distal-delta-front (55)	14,319–17,676	0.80–16.50	6.12
Distal-shoreline	Middle shoreface/medial-delta-front (82)	14,037–18,171	1.70–26.00	8.98
Proximal-shoreline	Upper-shoreface/proximal-delta-front (201)	14,017–18,183	1.60–26.30	14.21
Proximal-shoreline	Transgressive deposits (9)	14,084–16,109	8.00–24.70	16.50

Table 3. Summary of permeability data for each principal depositional facies listed in Table 1.

Depositional Systems	Facies (n)	Depth Range (ft)	Permeability Range (md)	Average Permeability (md)
Distal-shoreline	Lower shoreface/distal-delta-front (27)	14,319–16,088	0.010–1.800	0.140
Distal-shoreline	Middle shoreface/medial-delta-front (52)	14,037–16,486	0.010–5.190	0.371
Proximal-shoreline	Upper-shoreface/proximal-delta-front (198)	14,017–18,183	0.010–85.000	3.555
Proximal-shoreline	Transgressive deposits (9)	14,084–16,109	0.040–18.000	2.804

cation in these facies typically consists of starved ripples and low-angle, wavy laminae interbedded with burrowed mudstone beds within upward-coarsening successions. Ichnofauna are commonly dominated by *Planolites* with minor *Asterosoma*, *Teichichnus*, with minor *Ophiomorpha* within a *Cruziana* suite (Seilacher, 1964; Frey et al., 1990; Bromley and Asgaard, 1991; Benton and Harper, 1997; Anderson and Droser, 1998). Climbing ripples and thin, erosion-based and parallel-bedded sandstones with wavy and convex upper surfaces record periods of strong wave and/or storm activity.

Stronger storms are recorded by zones of broken and disrupted sandstone beds with mudstone clasts and shell fragments, similar to tempestite deposits described by Myrow and Southard (1996). Heavily burrowed strata alternating with sparsely burrowed zones with pyrite nodules reflect fluctuating conditions of salinity and oxygenation (MacEachern et al., 2005). Sharp-based, parallel-laminated sandstone beds and zones of contorted strata in the lower part of upward-coarsening sections record distal-deltaic turbidites representing rapidly deposited frontal splays associated with deltaic headlands (Mulder et al., 2003; Petter and Steel, 2006; Bhattacharya and MacEachern, 2009).

Shell No. 1–R Leyendecker

Description

A typical section in distal-shoreline systems occurs in the Shell No. 1–R Leyendecker well from 14,340 to 14,411 ft (4372.0 to 4393.6 m) (Fig. 3). The Shell No. 1–R Leyendecker well is located in the western part of Fandango Field, approximately 1000 ft (305 m) east of the main bounding growth fault (Fig. 2). According to Comstock Resources, Inc., the well has produced 23.8 Bcf (billion cubic feet) of gas collectively from three reservoirs (R, T3, and T6U [Fig. 2]).

Thickest and coarsest sandstone beds in the Shell No. 1–R Leyendecker well are up to 2 ft (0.6 m) thick, are fine-grained, and occur at the top of the section (Fig. 3). Many thin, very fine-grained sandstone beds in this core have an erosional base, are sparsely burrowed with minor *Planolites*, and are either internally laminated or have small-scale ripples (Figs. 4A and 4B). Thicker and coarser-grained sandstone beds in the succession have larger-scale, cross-cutting ripple scours above an erosional base. Infauna in these thicker sandstone beds are represented mainly by *Ophiomorpha* (Fig. 4C).

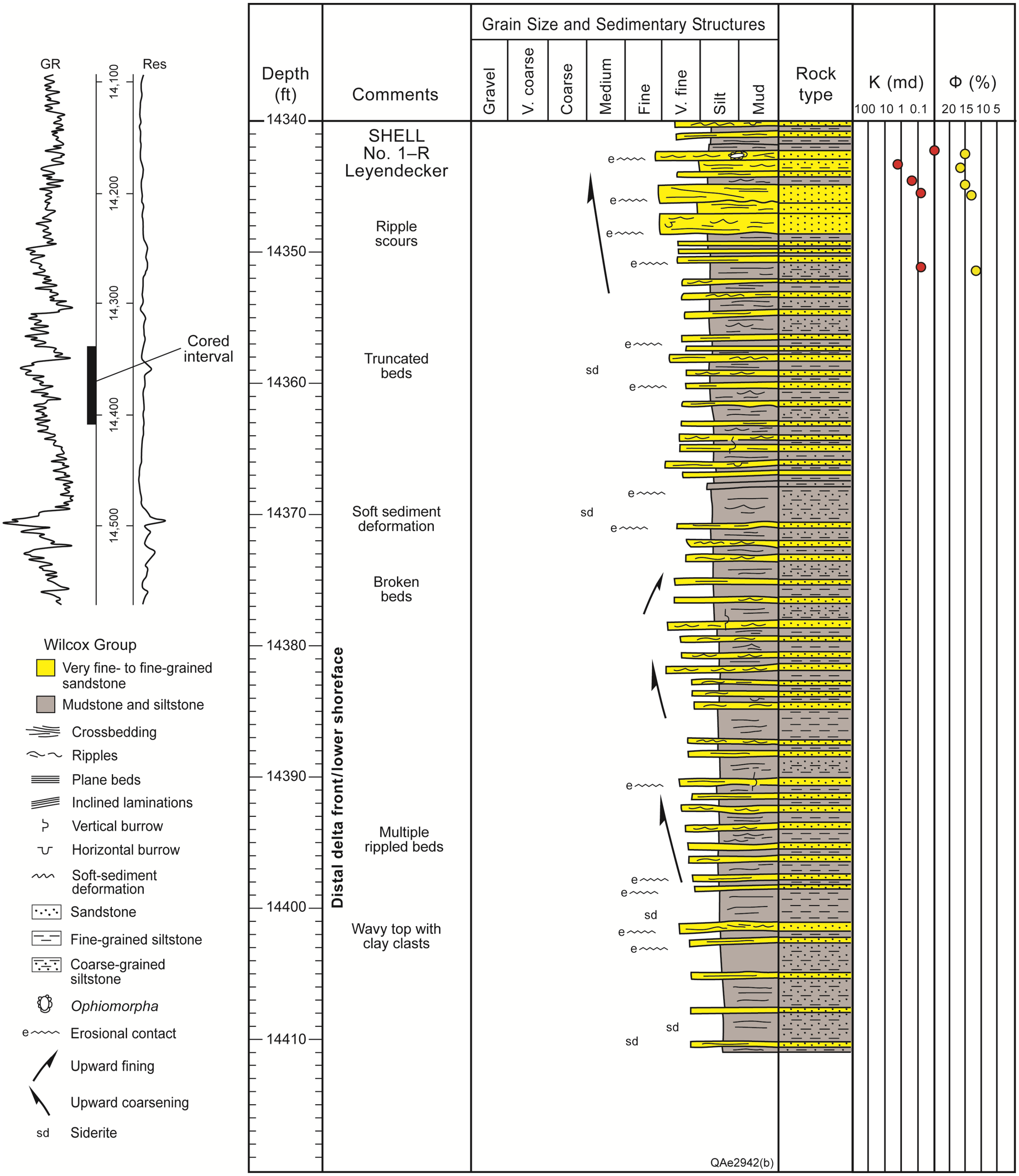

Figure 3. Core description and reservoir quality (permeability and porosity) data for the Shell No. 1–R Leyendecker well from 14,340 to 14,411 ft (4372.0 to 4393.6 m) in Fandango Field, Zapata County. Location of well is shown in Figure 2.

Interpretation

The Shell No. 1–R Leyendecker well is a muddy succession of distal-delta-front/lower-shoreface deposits. Fair-weather depositional processes in this succession are recorded in thin (commonly <4 in [<10.2 cm]) beds of laminated and ripple-stratified, very fine-grained sandstone beds (Figs. 4A and 4B). Higher-energy deposits recording wave-reworking are represented by erosion-based beds of cross-cutting ripples in fine-grained

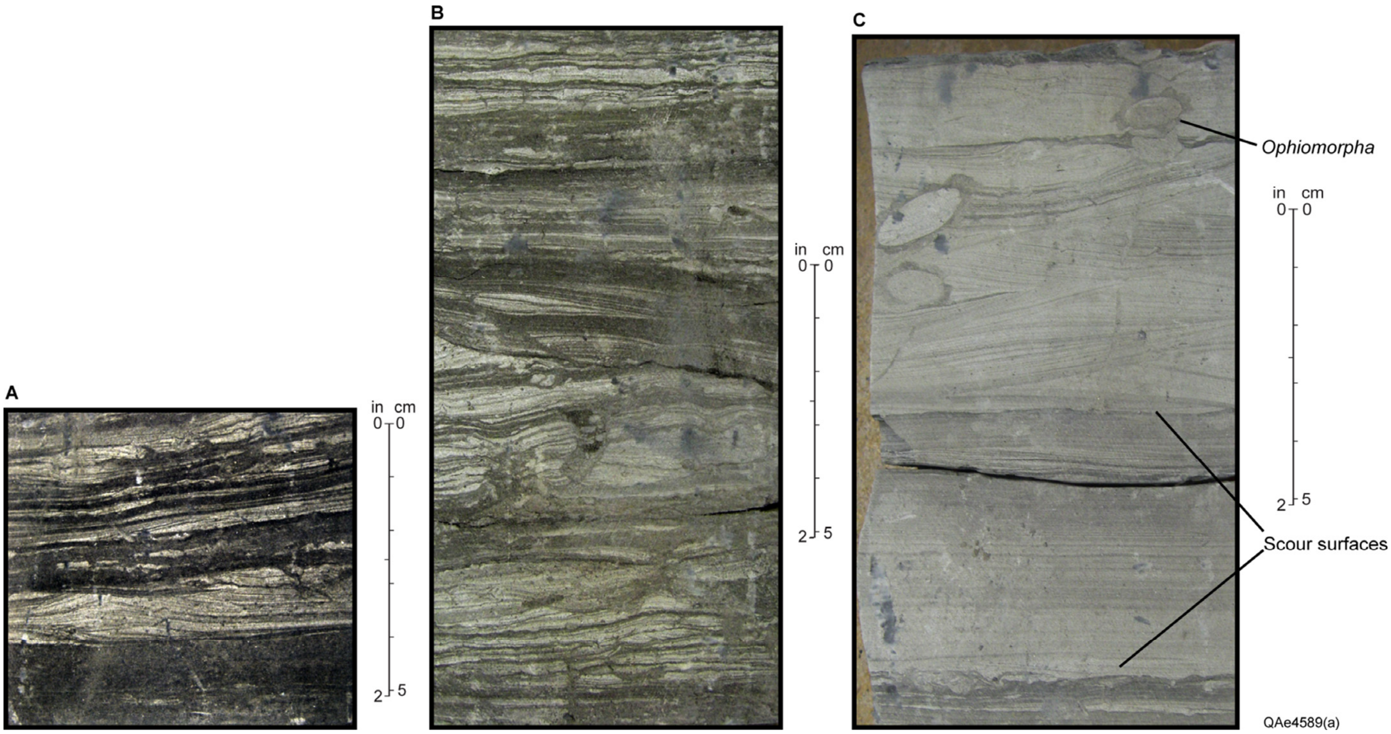

Figure 4. Photographs of lower-shoreface/distal-delta-front facies in the Shell No. 1–R Leyendecker well. (A) Ripple-stratified, very fine-grained sandstone interbedded with mudstone at 14,393.2 ft (4388.2 m). (B) Discontinuous, lenticular and laminated beds of very fine-grained sandstone at 14,357.2 ft (4377.2 m). (C) Cross-cutting ripple stratification in scour-based beds of fine-grained sandstone with *Ophiomorpha* burrows at 14,343.3 ft (4373.0 m). Core description is shown in Figure 3.

sandstone with *Ophiomorpha* burrows (Fig. 4C). Because of the preponderance of these thin (commonly <4 in [<10.2 cm]) beds of very fine- to fine-grained sandstone interbedded with relatively thicker beds of silty mudstone, the overall stratigraphic succession in the Shell No. 1–R Leyendecker well represents a low-energy, distal-delta-front or lower-shoreface setting.

Low-energy conditions with predominant suspension sedimentation in the distal-delta-front/lower-shoreface facies are recorded by mostly mudstone (Fig. 3). Thin (commonly <4 in [<10.2 cm]) sandstone beds in this succession record multiple episodes of turbidites in rapidly deposited splays, commonly expressed as sharp-based, parallel-laminated sandstone beds and zones of contorted strata on the unstable delta front substrate (Allison and Neill, 2002; Mulder et al., 2003; Neill And Allison, 2005; Petter and Steel, 2006; Bhattacharya and MacEachern, 2009).

Shell No. 1 Muzza

Description

The Shell No. 1 Muzza, located in the central part of Fandango Field, has produced 22.5 Bcf of gas collectively from the T2, T3, and T5 reservoirs (Comstock Resources, Inc., 2016, personal communication) (Fig. 2). A cored interval in this well, which spans 13,724 to 13,784 ft (4184.1 to 4202.4 m), is slightly upward coarsening. It ranges from lower-fine-grained sandstone with low-angle, planar and sparse ripple stratification with soft-sediment deformation to upper-fine-grained sandstone with *Palaeophycus*, *Planolites*, and minor *Ophiomorpha* and *Teichichnus* burrows (Fig. 5). Stratification in the lower part of the cored interval, where preserved, consists of ripples and low-angle plane beds (Fig. 6A). *Palaeophycus* burrows are the most common throughout the section (Figs. 6B and 6C). Stratification in the upper one-third of the cored interval is poorly preserved, as a result of abundant burrows (Fig. 6C).

Interpretation

The cored interval in the Shell No. 1 Muzza well records middle-shoreface facies grading upward into upper-shoreface facies in the top 5 ft (1.5 m) of the cored interval. This interpretation is based on: (1) a relatively coarser grain size than lower-shoreface deposits in the Shell No. 1–R Leyendecker core, where numerous mudstone beds are present (Fig. 3); (2) sparse number of zones with preserved stratification, consisting mostly of ripples; and (3) a high degree of bioturbation with ichnofauna dominated by *Palaeophycus*, *Planolites*, *Schaubcylindrichnus*, and *Asterosoma,* with minor *Ophiomorpha* (Fig. 5). The presence of *Schaubcylindrichnus* and *Asterosoma* suggests a low-energy, middle shoreface setting as opposed to a high-energy upper-shoreface to beach setting with high wave energy (Seilacher, 1964; Frey et al., 1990; Bromley and Asgaard, 1991; Benton and Harper, 1997; Gani et al., 2008).

PROXIMAL-SHORELINE SYSTEMS

Sandy, wave-dominated coastal systems, which include beach, upper-shoreface, and proximal-delta-front facies, are composed typically of well sorted and continuous, strike-elongate sandstone bodies. These systems are internally homogeneous as a result of their high-energy, shallow-marine depositional origin. Barrier-island systems are similar to beach systems, except that they consist of elongate, shore-parallel sand bodies separated from the shoreline by muddy lagoons. Strandplain deposits, also related to beach deposits, are composed of parallel, sandy beach ridges landward of the shoreline, reflecting individual episodes of coastal progradation (Curray et al., 1969; Hoyt, 1969; Dominguez et al., 1987).

The texture and degree of sandiness of beach deposits are a function of the beach profile, typically consisting of a gently sloping substrate in the transition from nearshore to offshore. Areas of intermediate water depth consist of the foreshore

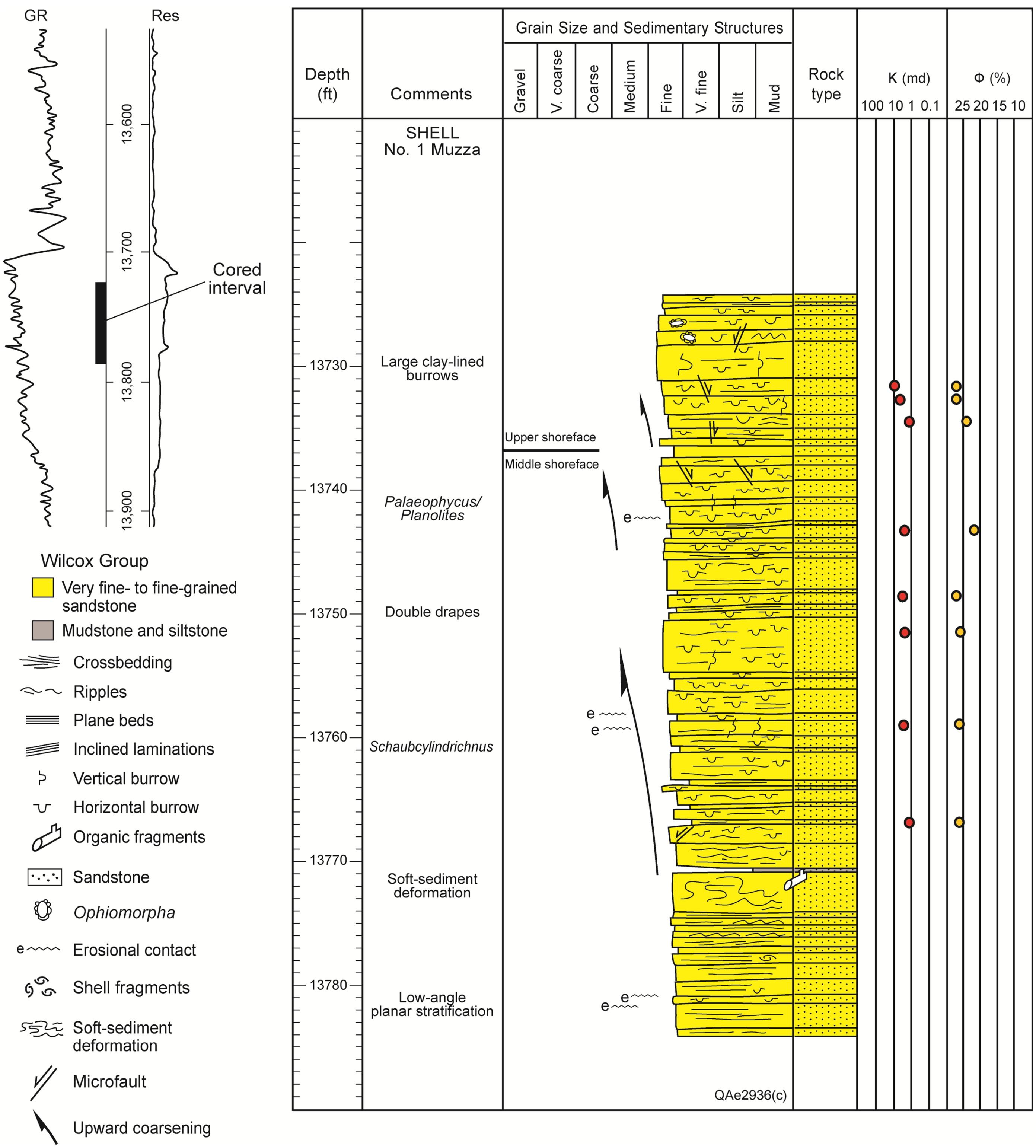

Figure 5. Core description and reservoir quality (permeability and porosity) data for the Shell No. 1 Muzza well from 13,724 to 13,784 ft (4184.1 to 4202.4 m) in Fandango Field, Zapata County. Location of well is shown in Figure 2.

(beach) and upper shoreface (mean water depth of <6.6 ft [<2 m]) (Howard and Reineck, 1972; Hill and Hunter, 1976). The foreshore and upper-shoreface environments are the sandiest parts of the system, which together compose the beach or barrier core. These environments are exposed to high-energy wave processes that winnow fine-grained material, resulting in relatively sandy, homogeneous deposits.

North American examples of modern shoreface, barrier-island, and strandplain deposits include Galveston Island in southeast Texas (Bernard et al., 1962), Padre Island in South Texas (Dickinson, 1971), the Nayarit strandplain along the western coastline of Mexico (Curray et al., 1969), and the wave-dominated shoreline along the Santee Delta in South Carolina (Stephens et al., 1976; Hodge, 1981). Galveston Island is an

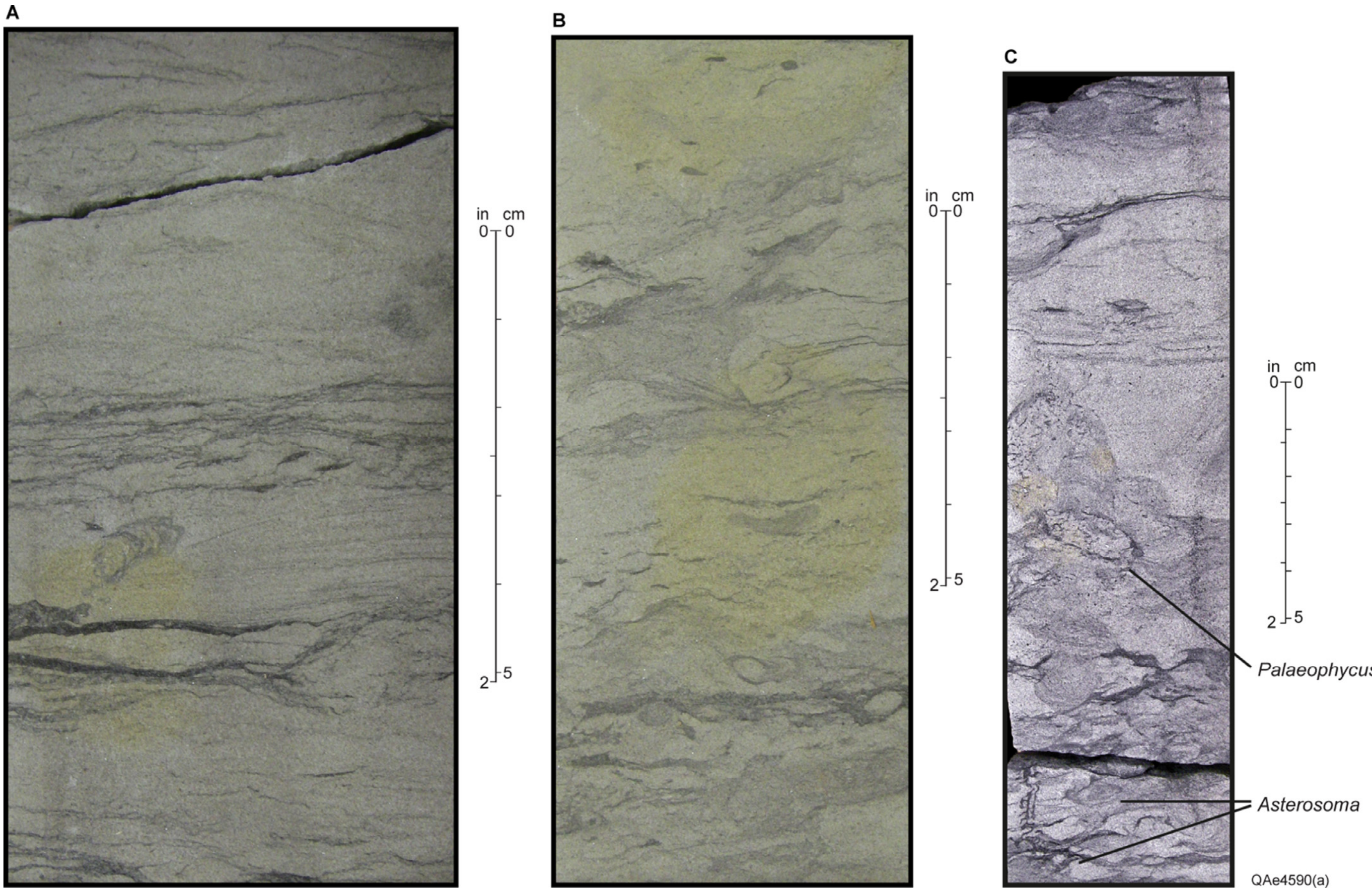

Figure 6. Photographs of middle-shoreface facies in the Shell No. 1 Muzza well. (A) Thin (<1 in [<2.5 cm]) beds of planar-stratified, ripple-laminated, and burrowed fine-grained sandstone at 13,769.6 ft (4198.0 m). Prominent burrow in lower part of photograph is *Teichichnus*. (B) Extensively burrowed, fine-grained sandstone with dominantly *Palaeophycus* burrows at 13,767.8 ft (4197.5 m). (C) Burrowed, upper very fine-grained sandstone overlain by sparsely burrowed, fine-grained sandstone at 13,743.0 ft (4189.9 m). Core description is shown in Figure 5.

example of a progradational barrier island that has migrated offshore during the Holocene as a result of sediment supply exceeding subsidence and/or rise in sea level (Bernard et al., 1962). Cross sections of Galveston Island exhibit an upward-coarsening grain-size trend from lower shoreface to eolian dune facies. Sandbody homogeneity and reservoir quality increase upward as a result of upper-shoreface facies being superimposed above lower-shoreface facies during episodes of coastal offlap (Bernard et al., 1962). Although beach deposits contain tabular, laterally continuous, and homogeneous sandstone bodies, they are commonly crosscut by tidal-inlet and distributary-channel deposits that introduce facies heterogeneity and permeability contrasts, as for example in the 41–A reservoir in the Oligocene Frio West Ranch Field in Jackson County, Texas (Galloway and Cheng, 1985; Galloway, 1986).

The Santee Delta is an example of a wave-dominated shoreline depositional system, where shore-parallel, sandy-beach, and upper-shoreface deposits are locally transected by a tidally influenced distributary channel. Other areas of facies heterogeneity in the Santee Delta and adjacent areas along the South Carolina shoreline occur along landward pinchouts of lobate washover fans, and transgressive beach escarpments (Ruby, 1981), Facies heterogeneity is also controlled by tidal inlets and ebb- and flood-tidal deltas that locally bisect the shoreline (Swift, 1968; Kumar and Sanders, 1976; Hayes, 1979; Kraft and John, 1979; Reinson, 1984).

Shell No. 1 Garza

Description

The non-productive Shell No. 1 Garza well is located on the southern margin of Fandango Field (Fig. 2). A cored interval in the Shell No. 1 Garza well, which extends from 16,190 to 16,265 ft (4936.0 to 4958.8 m), consists of a 75-ft (22.9-m) sandstone-rich section of predominantly fine-grained sandstone within an interval characterized by a blocky GR log response (Fig. 7). This sandy section contains numerous sandstone-on-sandstone contacts with erosional surfaces. Individual sandstone beds in the section range in thickness from 1 to 3 ft (0.3 to 0.9 m). Two main types of strata in the section consist of burrowed, upper very fine- to fine-grained sandstone dominated by *Ophiomorpha* and *Planolites* (Figs. 8A and 8B) and planar-stratified, fine-grained sandstone with *Ophiomorpha* burrows (Fig. 8C).

Interpretation

This sandy interval in the Shell No. 1 Garza core (Fig. 7) is composed of aggradational, upper-shoreface facies in a wave-dominated depositional setting, analogous to similar facies in the Upper Pictured Cliffs Sandstone in the San Juan Basin (Ayers et al., 1994; Ambrose and Ayers, 2007). The Upper Pictured Cliffs Sandstone records high-frequency, Late Cretaceous transgressive-regressive episodes composed of amalgamated barrier-strandplain sandstone-bodies in individual successions up to 100

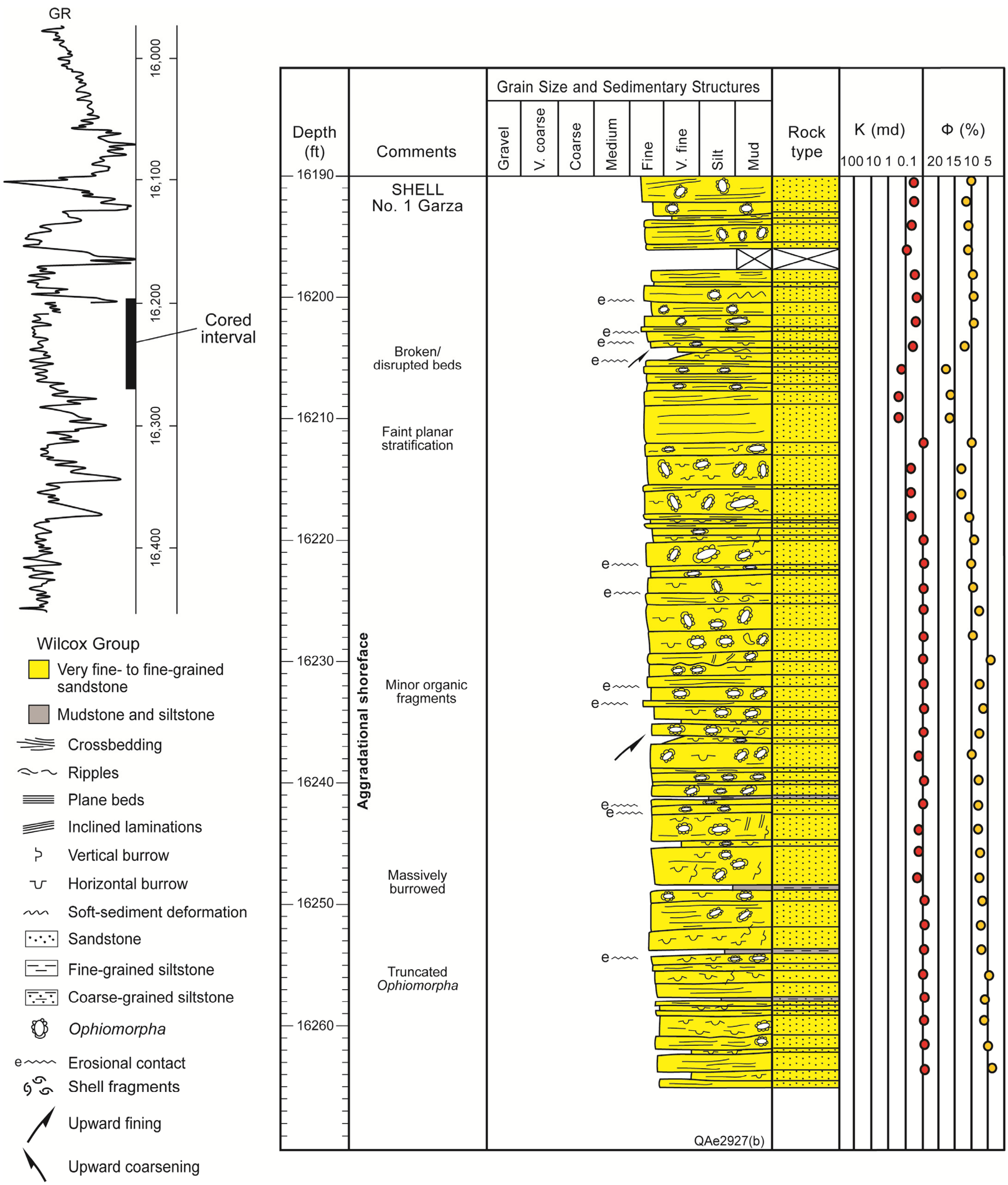

Figure 7. Core description and reservoir quality (permeability and porosity) data for the Shell No. 1 Garza well from 16,190 to 16,265 ft (4936.0 to 4958.8 m) in Fandango Field, Zapata County. Location of well is shown in Figure 2.

ft (30 m) thick. These amalgamated sandstone bodies have a net blocky vertical grain-size profile similar to that of the overall stratigraphic succession in the Shell No. 1 Garza core, where the vertical grain-size profile is almost uniformly fine- to upper-fine-grained (Fig. 7). The Pictured Cliffs Sandstone typically has a blocky to upward-coarsening well-log response and is composed of amalgamated sandstone bodies having a composite thickness of 40 to 120 ft (12 to 36 m). It is inferred to be the framework

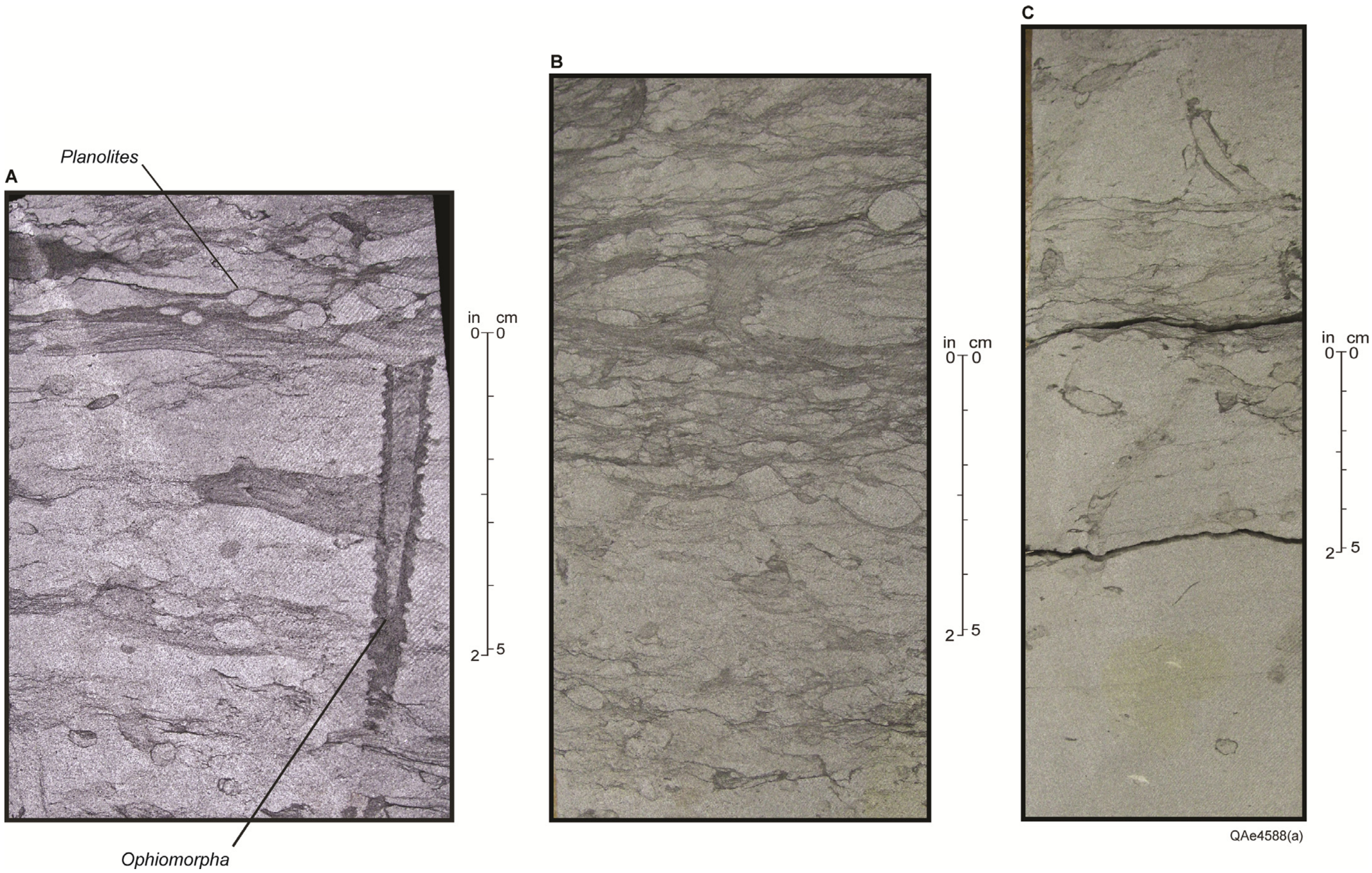

Figure 8. Photographs of amalgamated upper-shoreface facies in the Shell No. 1 Garza well. (A) Truncated *Ophiomorpha* burrow in fine-grained sandstone at 16,254.2 ft (4955.6 m). Other burrows are dominated by *Planolites*. (B) Extensively burrowed, very fine-grained sandstone at 16,237 ft (4950.3 m). (C). Low-angle planar-stratified, fine-grained sandstone with *Ophiomorpha* burrows at 16,225 ft (4946.6 m). Core description is shown in Figure 7.

facies of prograding barrier-strandplain or wave-dominated delta depositional systems (Fassett and Hinds, 1971; Erpenbeck, 1979; Cumella, 1981; Flores and Erpenbeck, 1981; Cumella, 1983; Manfrino, 1984, Ambrose and Ayers, 1990; Ayers et al., 1994).

A steeply dipping, 300 ft (~90 m) section of the Pictured Cliffs Sandstone is exposed along Colorado State Highway 3 on the southeast edge of Durango, Colorado (Fig. 9A). The main portion of this continuous outcrop displays a 200 ft (60 m) succession of shelf mudstones and thin, very fine- to fine-grained sandstones in the Lewis Shale that grades upward into fine-grained, wave-dominated shoreface deposits in the Pictured Cliffs Sandstone, forming the top of the steeply dipping cliff in Fig. 9A. This section is well-documented in previous studies of the Lewis Shale to Fruitland succession, including Condon et al. (1997), Fassett (2000), and Ambrose and Ayers (2007). Individual Pictured Cliffs sandstone beds in this outcrop are typically sharp-based. Stratification is dominated by low-angle and horizontal laminations as well as large-scale, concordant and wavy bedding overlain by ripples and plane beds. Burrows are common, consisting mainly of *Ophiomorpha* (Fig. 9B), consistent with predominant *Ophiomorpha* in the Shell No. 1 Garza core (Figs. 8A, 8C, and 9B). The sets of large-scale wavy beds represent hummocky stratification recording storm events in a shoreface setting similar to that described by Dott and Bourgeois (1982). Similar successions of sandstones with scoured bases overlain by hummocky-stratified, fine-grained sandstone ~8 to 20 in (20 to 50 cm) thick, in turn overlain by ripple- to planar-laminated, bioturbated, very fine-grained sandstone are also observed in the Pictured Cliffs Sandstone by Tokar and Evans (1993). They interpret the Pictured Cliffs Sandstone south of Durango to have been deposited on a storm-dominated, sandy shelf at depths between fair-weather and storm-weather wave-base (~30 ft [~10 m]).

Shell No. 2 Muzza

A core in the Shell No. 2 Muzza well illustrates two sandy, upward-coarsening shoreface parasequences (Fig. 10). This well is located on the northwestern margin of Fandango Field, closely downdip (east) of the main bounding fault in the field (Fig. 2). The Shell No. 2 Muzza well has produced 47.1 Bcf of gas from the R and T6U reservoirs, according to Comstock Resources, Inc.

Description

The cored interval in the Shell No. 2 Muzza well extends from 15,588 to 15,640 ft (4752.4 to 4768.3 m) (Fig. 10). The section consists of two upward-coarsening intervals, the lower ranging from 15,619 to approximately 10 ft (3 m) below the base of the core, based on the GR log response 15,651 ft (4761.9 to 4771.6 m), and the upper extending from 15,588 to 15,619 ft (4752.4 to 4761.9 m) (Fig. 10). The lower upward-coarsening interval ranges from ripple- and planar-stratified, the upper interval ranges from very fine-grained sandstone at the base to burrowed, fine-grained sandstone (Fig. 11A) to fine-grained, planar-stratified sandstone with small (2 to 4 mm diameter) clay clasts at the top. This upward-coarsening interval is overlain by a 4 ft (1.2 m) muddy section that contains millimeter- and centimeter-scale beds of contorted and sparsely burrowed, very fine-grained sandstone (Fig. 11B). The upper upward-coarsening interval above

Figure 9. (A) Steeply dipping outcrop along Colorado State Highway 3 southeast of Durango, Colorado, displaying the Lewis Shale in gradational contact with the overlying Pictured Cliffs Sandstone, composed of aggradational shoreface deposits in a wave-dominated depositional setting, an analog for amalgamated upper-shoreface deposits in the cored interval in the Shell No. 1 Garza well (Fig. 7). (B) *Ophiomorpha* burrows in the Pictured Cliffs Sandstone, with location of photograph indicated in Figure 9A.

this muddy section grades upward from very fine-grained, ripple-laminated sandstone to fine-grained, unburrowed, and planar-stratified sandstone with thin (millimeter-scale) and discontinuous lenses of muddy and organic material (Fig. 11C).

Interpretation

The Shell No. 2 Muzza core encompasses the most part of two progradational, wave-dominated, shoreface parasequences (Fig. 10). The upper 2 ft (0.6 m) of the lower parasequence is composed of upward-fining, transgressive deposits above an inferred transgressive surface of erosion at 15,620 ft (4762.2 m) (Fig. 10). This inferred transgressive surface of erosion is recognized in the Shell No. 2 Muzza core by: (1) an erosional surface overlain by mud clasts; and (2) a change in grain size from fine to fine-to-medium grained sandstone (Fig. 10).

Multiple scour surfaces at the base of planar-stratified sandstone beds in the middle and upper parts of these parasequences record intermittent periods of high-energy, longshore-drift processes that truncate burrowed beds of upper very fine- to lower fine-grained sandstone that were deposited during periods of quiescence. Similar stratigraphic architecture occurs in the Campanian Upper Pictured Cliffs Sandstone in the San Juan Basin (Ambrose and Ayers, 2007) as well as upper-offshore facies in the modern Sapelo Island, Georgia (Howard and Reineck, 1972).

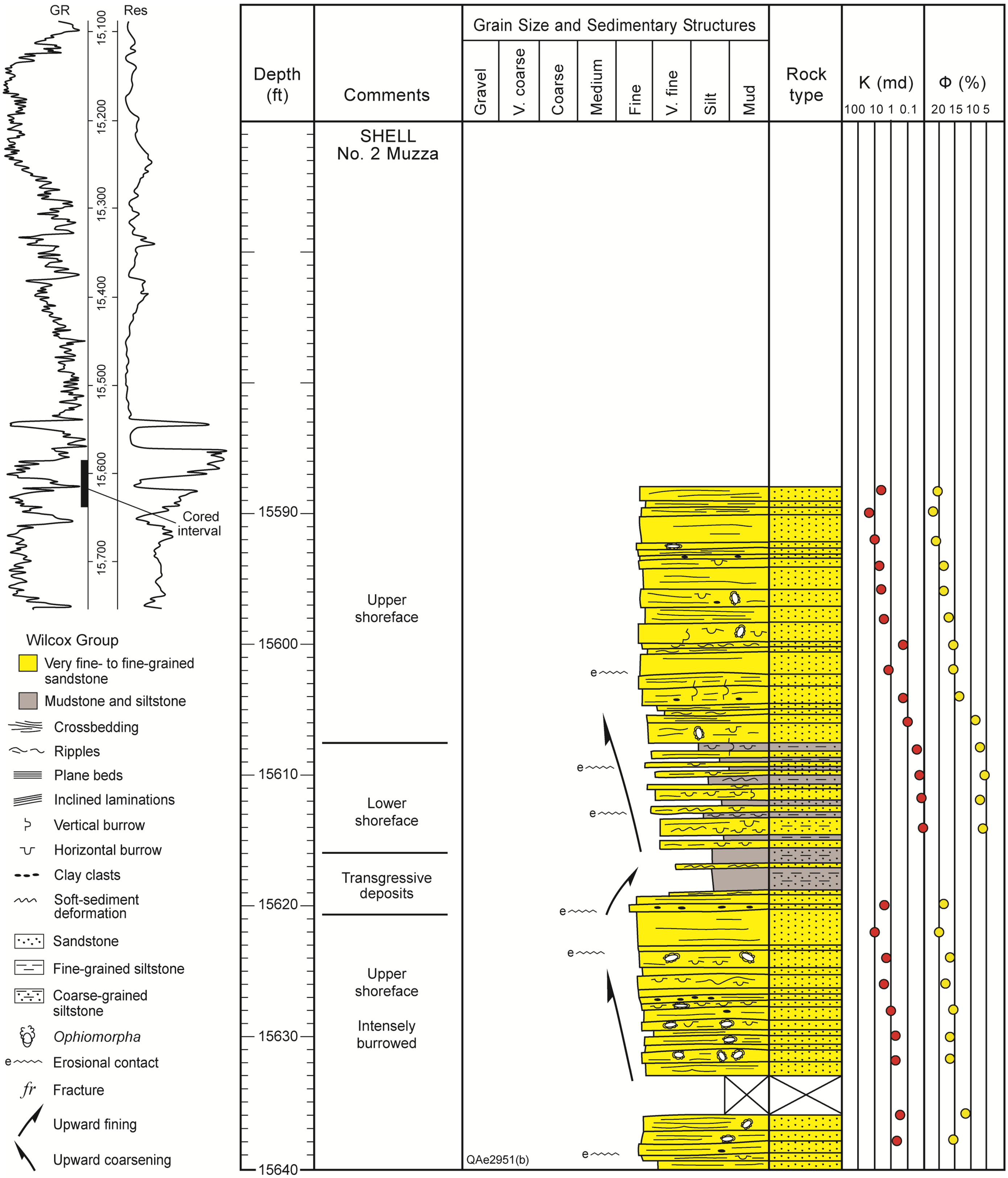

Figure 10. Core description and reservoir quality (permeability and porosity) data for the Shell No. 2 Muzza well from 15,588.0 to 15,640.0 ft (4752.4 to 4768.3 m) in Fandango Field, Zapata County. Location of well is shown in Figure 2.

Shell No. 3 Hinojosa

Description

The Shell No. 3 Hinojosa well is located on the southeastern margin of Fandango Field and is classified as a non-productive, water-wet well (Fig. 2). The cored interval, which is at the top of a thick (≥140 ft [≥43 m]) section with a complex GR response (upward-coarsening to serrate), is an upward-coarsening section that ranges from upper very fine-grained sandstone at the base to fine-grained sandstone at the top (Fig. 12). Stratification in the

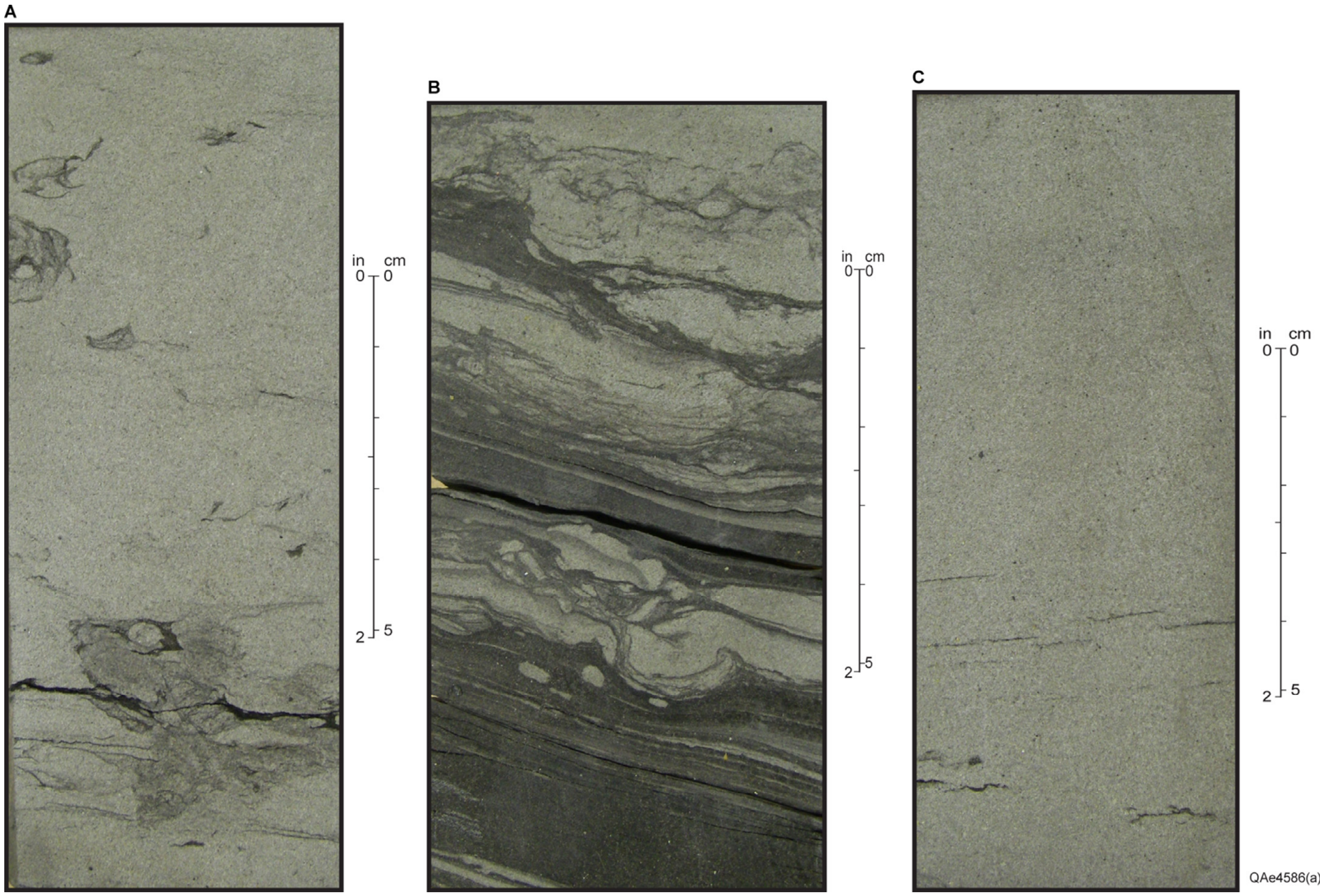

Figure 11. Photographs of predominantly upper- and lower-shoreface facies from the Shell No. 2 Muzza well. (A) Burrowed, fine-grained sandstone at 15,629.0 ft (4764.9 m) in upper-shoreface facies. (B) Very fine-grained sandstone with load structures at 15,614.3 ft (4760.5 m) in lower-shoreface facies. (C) Fine-grained sandstone with low-angle planar stratification at 15,602.4 ft (4756.8 m) in upper-shoreface/beach facies. Core description is shown in Figure 10.

lower 10 ft (3 m) of the section is dominated by low-angle planar bedsets with rare vertical escape burrows (Fig. 13A), whereas the upper 40 ft (12 m) contains either horizontal to low-angle inclined planar stratification, crossbedding, and massive bedding (Fig. 13B). The section also contains numerous, subtle scour surfaces that separate smaller sections ranging in thickness from 3 to 10 ft (1.5 to 4.5 m) (Fig. 12).

Interpretation

This cored interval in the Shell No. 3 Hinojosa well consists of a lower, 10 ft (3 m) section of very fine- to fine-grained sandstone in inner-shelf facies dominated by zones of swaley stratification (Fig. 13A). In contrast, the upper 20 ft (6 m) of the cored interval is composed of fine-grained, massive to faintly planar-stratified sandstone recording upper-shoreface deposits (Figs. 12 and 13B). High wave energy in the upper one-third of the cored section is inferred from the amalgamated succession of multiple, 3 to 10 ft (1.5 to 4.5 m) erosion-based zones, planar-stratified and crossbedded sandstone beds. This type of stratification is common in wave-dominated successions that record multiple episodes of sediment transport by longshore drift and welding of beach-ridge deposits (Pilkey and Davis, 1987; Walker and Plint, 1992). Modern depositional analogs include prograding beach-ridge deposits in Kiawah Island in South Carolina (Barwis, 1976) and progradational barrier-island deposits in Galveston Island in Texas, where the upper 10 to 16 ft (3 to 5 m) consists of unburrowed, cross-stratified and planar-stratified, fine-grained sand (Bernard et al., 1962; Davies et al., 1971).

RESERVOIR QUALITY

Crossplots of grain size, expressed in terms of ϕ units, versus permeability and porosity, indicate that facies origin is a poor predictor or reservoir quality in the upper Wilcox succession in Fandango Field. Crossplots of grain size versus both permeability and porosity data from all data points in this study, have coefficient of determination (R^2) values of 0.3276 and 0.4696, respectively (Figs. 14A and 14B, respectively). The distribution of permeability values for all data points displays a large population of low permeability values <10 md (266 data points) and a small population (20 data points) for values >10 md (Fig. 14A). In contrast, the distribution of porosity values for all data points is less skewed than that for permeability values. It is associated with a less-steep, best-fit trend line for relatively low values in comparison with the best-fit trendline for permeability values (Fig. 14B).

Crossplots of grain size versus permeability and porosity for individual facies (lower shoreface, middle shoreface, upper shoreface, and transgressive deposits) display great differences in terms of distribution of permeability and porosity values, R^2 values and geometry of trend lines (Figs. 15–18). Among these four facies types, transgressive deposits exhibit the highest R^2 values (0.9261 and 0.6792 for grain size versus permeability and porosi-

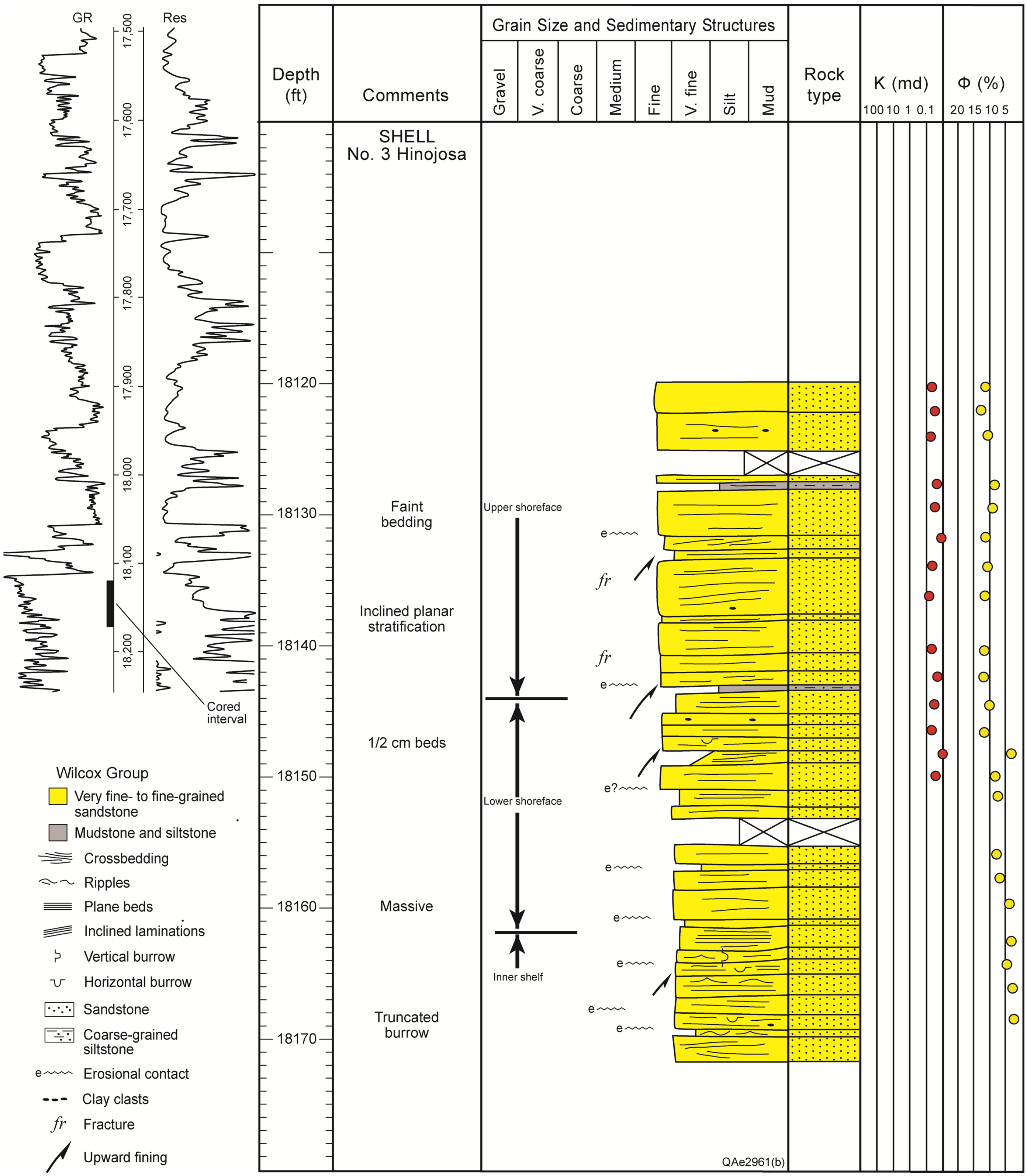

Figure 12. Core description and reservoir quality (permeability and porosity) data for the Shell No. 3 Hinojosa well from 18,120 to 18,171.5 ft (5524.4 to 5540.1 m). Location of well is shown in Figure 2.

ty [Figs. 18A and 18B, respectively]), although only nine data points represented transgressive deposits in the data set. Low R^2 values (<0.350) are associated with crossplots of grain size versus both permeability and porosity in lower-shoreface facies (Figs. 15A and 15B, respectively), grain size versus porosity in middle-shoreface facies (Fig. 16B), and grain size versus permeability and porosity in upper-shoreface facies (Fig. 17A). Higher R^2 values (0.5061) are associated with the crossplot of grain size versus permeability for middle-shoreface facies (Fig. 16A).

Although poor correlations exist between grain size and reservoir quality for these facies, differences in range and average values in reservoir quality do occur between some facies.

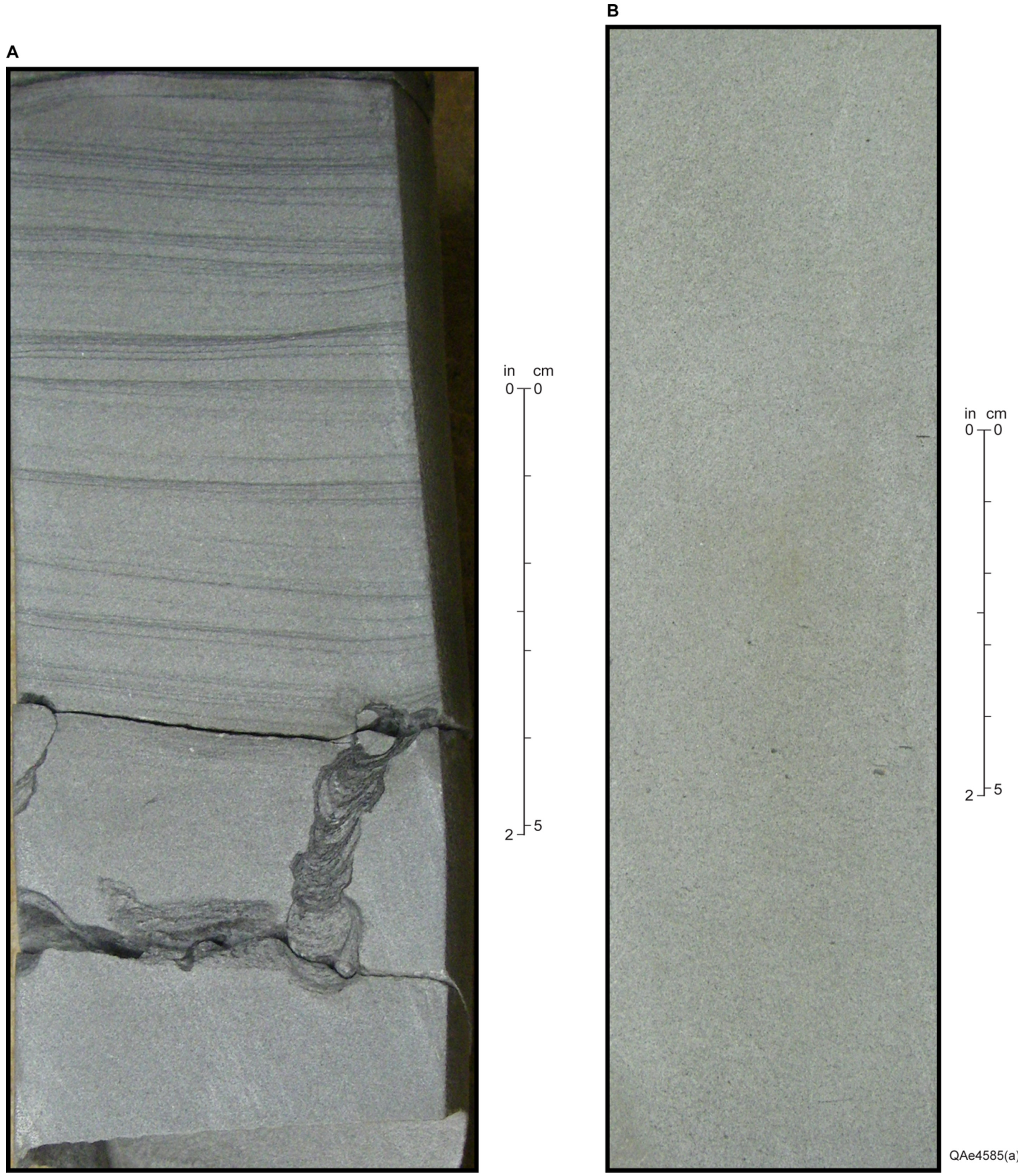

Figure 13. Photographs of shelf overlain by upper-shoreface facies from the Shell No. 3 Hinojosa well. (A) Low-angle swaley stratification and vertical escape burrow (*Teichichnus*) in very fine- to fine-grained sandstone at 18,162.6 ft (5537.4 m). Swaley stratification indicates deposition between fair weather and storm wave base in inner-shelf setting. (B) Massively bedded, fine-grained sandstone at 18,128.0 ft (5526.8 m) in upper-shoreface setting. Core description is shown in Figure 12.

Relatively high values of average porosity (14.21 to 16.50%) occur in proximal-shoreline depositional systems, whereas lower values (<9%) are within muddy distal-marine depositional systems (Table 2). Likewise, greater values of permeability are within nearshore/proximal-shoreline depositional systems, with average values of 3.555 and 2.804 md in upper-shoreface/proximal-delta-front and transgressive deposits, respectively (Table 3). In contrast, average permeability values are much lower (<0.400 md) in offshore/distal-shoreline depositional systems, with low values (average 0.140 md) in lower-shoreface/distal-delta-front facies. Although average values of permeability are comparable in upper-shoreface/proximal-delta-front and transgressive deposits, these facies differ greatly in terms of their highest values (85 versus 18 md) (Table 3).

Variations in porosity and permeability occur within the transition from lower- to upper-shoreface facies in some cores, whereas in other cores these relationships are poor. For example, in the Shell No. 1 Garza core, the greatest values of porosity and permeability occur near the top of two upward-coarsening successions, where values are as much as 22.5% and 20 md, respec-

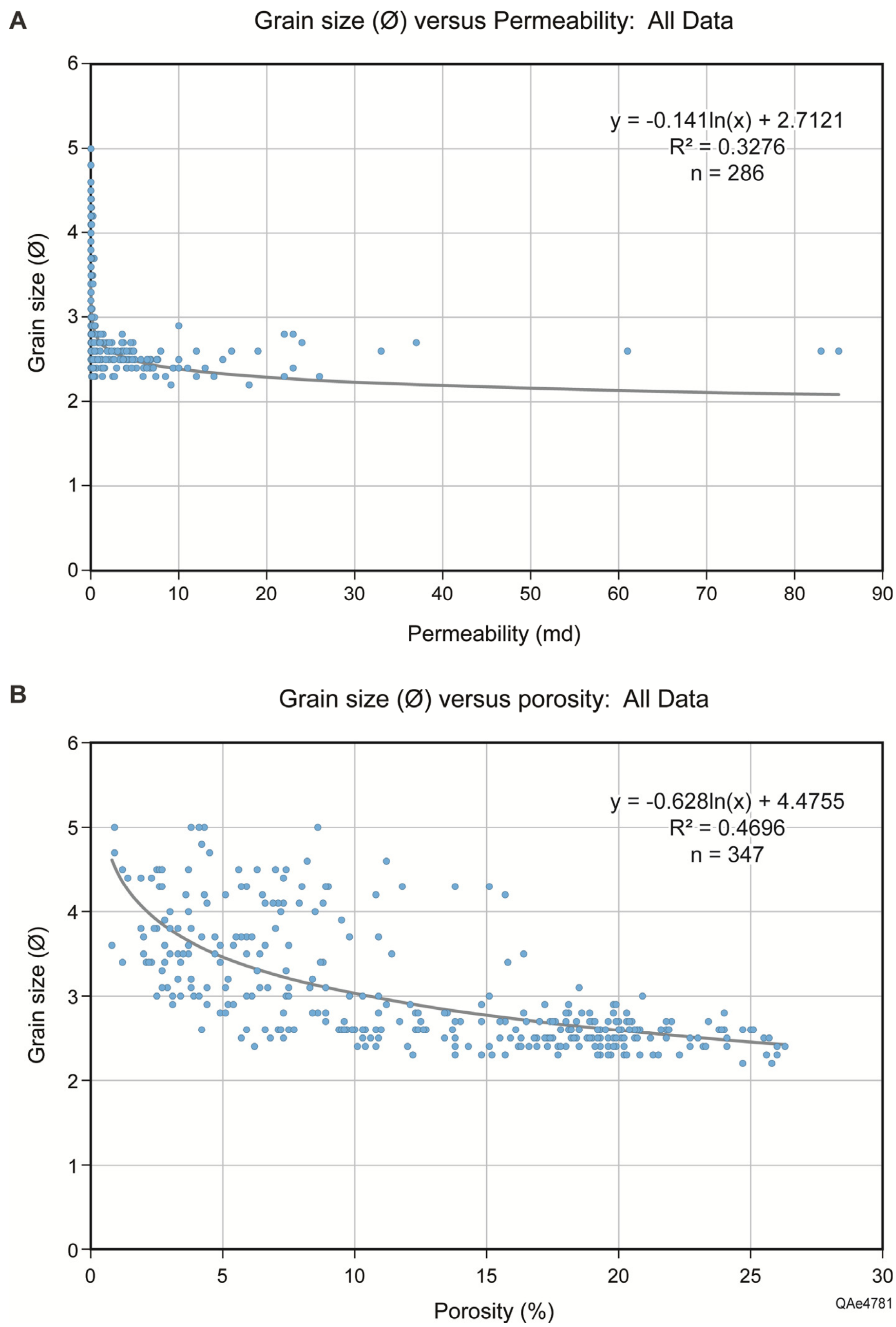

Figure 14. Grain size (ϕ units) versus reservoir-quality data for all whole-core plug data in this study. (A) Permeability and (B) Porosity.

tively (Fig. 10). Likewise, a slight upward increase in permeability values (although all values are <0.1 md) and porosity values (5.5 to 7.0%) occurs in lower-shoreface facies from 15,609 to 15,615 ft (4758.8 to 4760.7 m) in the Shell No. 2 Muzza well (Fig. 10). In addition, the transition from middle- to upper-shoreface facies in the Shell No. 1 Muzza core corresponds with a minor increase in permeability values from slightly >1 md to almost 10 md (Fig. 5). However, no corresponding upward increase in porosity values occurs in the same interval. Abundant permeability and porosity data in the Shell No. 1 Garza core indicate little net variation in reservoir quality over the entire cored succession, although subtle trends of upward-increasing and upward-decreasing values occur within smaller (5 to 20 ft [1.5 to 6 m]) intervals (Fig. 7). This interval in the Shell No. 3 Hinojosa well contains porosity data for the entire interval and permeability data from the upper 60% (Fig. 12). These data indicate an upward increase in porosity values from approximately 3 to 13% over the transition from inner-shelf to upper-shoreface facies, although permeability data are absent for the lower 20 ft (6 m).

CONCLUSIONS

This study presents a wave-dominated, microtidal (diurnal tidal range <6.6 ft [<2 m]) interpretation for the deeply-buried (>13,000 ft [>3960 m]) upper Wilcox Group in Fandango Field, based on presence of wavy, symmetrical ripples coupled with the absence of features that are common in tidally-modified or tide-dominated settings such as rhythmic stratification, lenticular

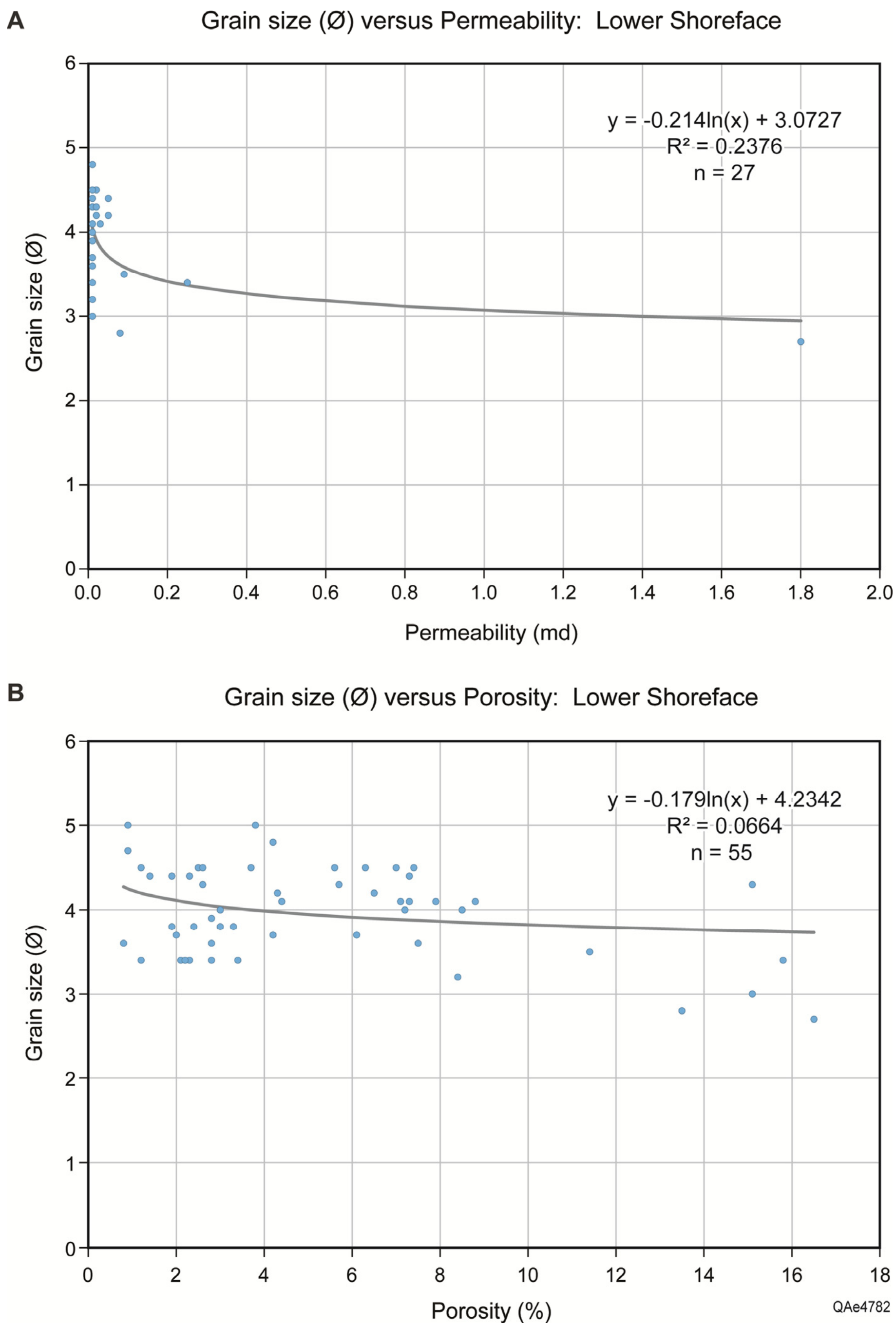

Figure 15. Grain size (ϕ units) versus reservoir-quality data for lower-shoreface facies. (A) Permeability and (B) Porosity.

beds, flaser ripples, and double-draped ripples. Modern depositional analogs for the upper Wilcox Group in Fandango Field include the wave-dominated Santee Delta and Cape Romain in South Carolina, whereas upper-shoreface and wave-dominated deltaic deposits in the upper Cretaceous (Campanian) Pictured Cliffs Sandstone in the San Juan Basin in New Mexico and Colorado serve as an ancient facies analog.

Crossplots of grain size versus porosity and permeability for the total dataset of 347 plugs from whole core indicate that grain size, and facies origin to a lesser extent, are poor predictors of reservoir quality (defined as porosity and permeability) in the upper Wilcox succession in Fandango Field. However, minor variation in reservoir quality exists between different shoreface and wave-dominated deltaic facies. Optimal reservoir quality occurs in sandy upper-shoreface/proximal-delta-front facies and transgressive deposits in Fandango Field. Relatively high values of average porosity (14.2 to 16.5%) occur in amalgamated, fine-grained sandstone beds in upper-shoreface/proximal-delta-front facies, whereas lower values (<9%) are prevalent in lower-shoreface/distal-delta-front facies. Similarly, greater values of permeability occur within upper-shoreface/proximal-delta-front and transgressive deposits, with average values of 3.56 and 2.80 md in upper-shoreface/proximal-delta-front and transgressive deposits, respectively. In contrast, average permeability values are much lower (0.14 md) in lower-shoreface/distal-delta-front facies.

This study shows that grain size and facies variability in the upper Wilcox succession in Fandango Field are poor indicators of reservoir quality. Although minor variation in range and average values of permeability and porosity exists between facies in

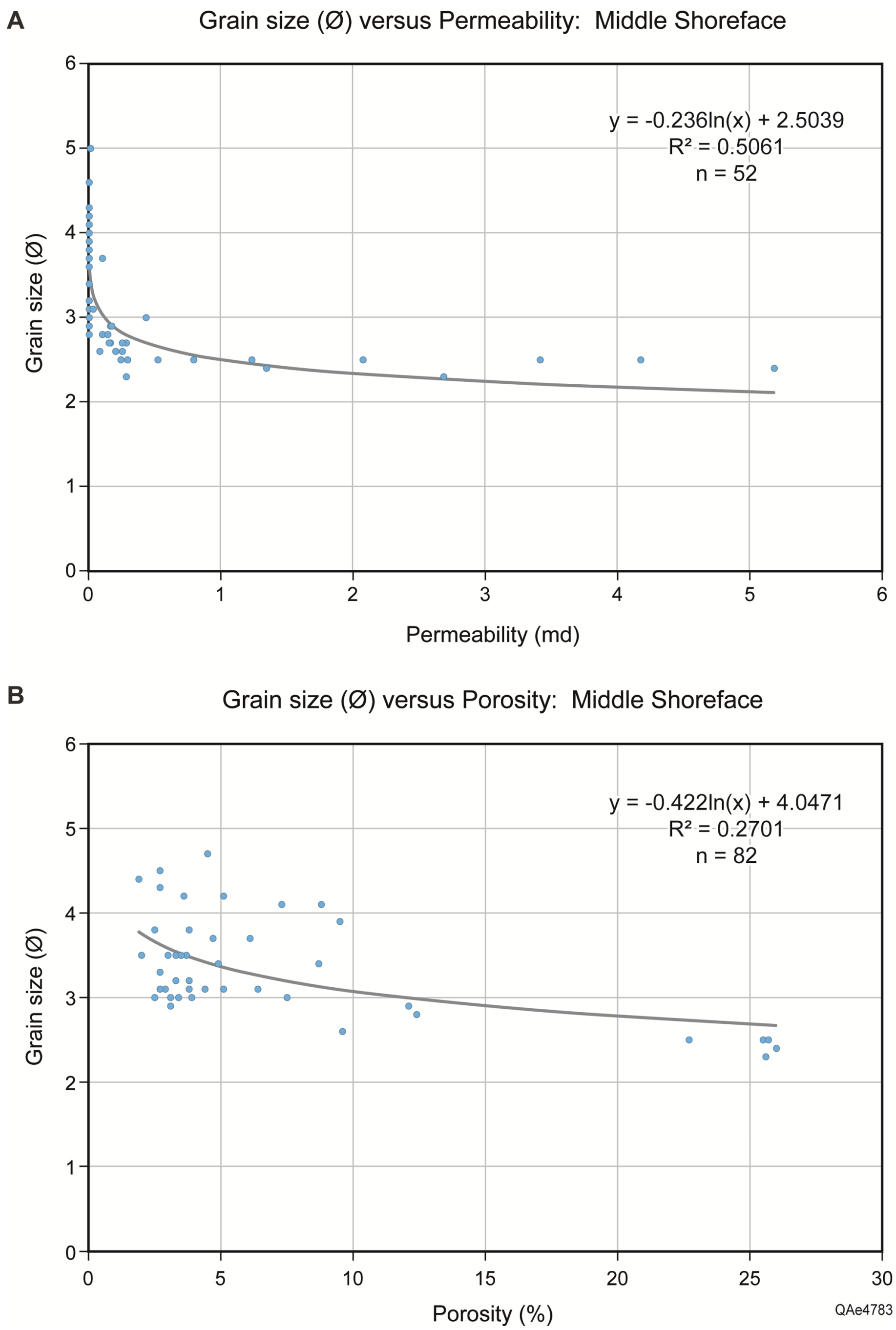

Figure 16. Grain size (ϕ units) versus reservoir-quality data for middle-shoreface facies. (A) Permeability and (B) Porosity.

Fandango Field, other factors such as diagenesis may control reservoir quality and should also be considered in reservoir development in neighboring Wilcox fields in South Texas.

ACKNOWLEDGMENTS

This study was funded by the Deep Shelf Gas Consortium at the Bureau of Economic Geology, University of Texas at Austin. Production data and structure map of Fandango Field were provided by Comstock Resources, Inc. The manuscript benefitted from the reviews of Erin Meyers and Tom Dunn. Francine Mastrangelo and Anastasio Grebnova prepared the illustrations under the direction of Cathy Brown, Manager, Media Information Technology. Publication authorized by the Director, Bureau of Economic Geology.

REFERENCES CITED

Allison, M. A., and C. F. Neill, 2002, Accumulation rates and stratigraphic character of the modern Atchafalaya River prodelta, Louisiana: Gulf Coast Association of Geological Societies Transactions, v. 52, p. 1031-1040.

Ambrose, W. A., 1990, Facies heterogeneity and brine-disposal potential of Miocene barrier-island, fluvial, and deltaic systems: examples from Northeast Hitchcock and Alta Loma fields, Galveston County: Texas Bureau of Economic Geology Geological Circular 90–4, Austin, 35 p.

Ambrose, W. A., and W. B. Ayers Jr., 1990, Barrier-strandplain deposits of the Pictured Cliffs Sandstone and coal occurrence in the Fruitland Formation, northern San Juan Basin, Colorado and New Mexico: American Association of Petroleum Geologists Bulletin, v. 74, p. 1313.

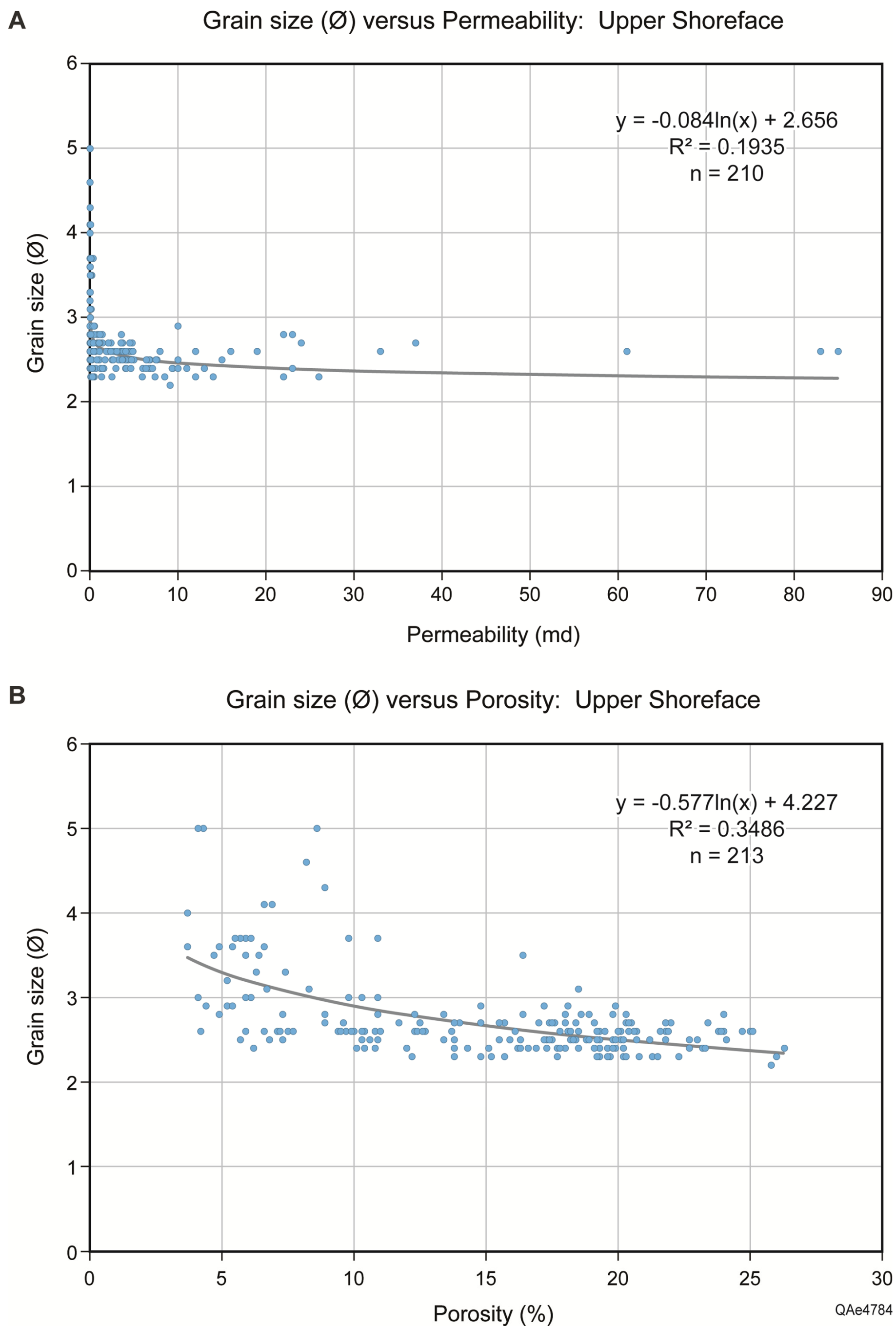

Figure 17. Grain size (ϕ units) versus reservoir-quality data for upper-shoreface facies. (A) Permeability and (B) Porosity.

Ambrose, W. A., and W. B. Ayers, Jr., 2007, Geologic controls on transgressive-regressive cycles in the upper Pictured Cliffs Sandstone and coal geometry in the lower Fruitland Formation, northern San Juan Basin, New Mexico and Colorado: Association of Petroleum Geologists Bulletin, v. 91, p. 1099–1122.

Ambrose, W. A., and T. F. Hentz, 2012, Shelf-edge deltaic depositional systems in the Upper Woodbine succession, Double A Wells Field, Polk County, Texas: Gulf Coast Association of Geological Societies Transactions, v. 52, p. 3–12.

Anderson, B. G., and M. L. Droser, 1998, Ichnofacies and geometric configurations of *Ophiomorpha* within a sequence stratigraphic framework: an example from the Upper Cretaceous US western interior: Sedimentology, v. 45, p. 379–396.

Ayers, W. B., Jr., W. A. Ambrose, and J. S. Yeh, 1994, Coalbed methane in the Fruitland Formation, San Juan Basin: Depositional and structural controls on occurrence and resources, *in* W. B. Ayers, Jr. and W. R. Kaiser, eds., Coalbed methane in the Upper Cretaceous Fruitland Formation, San Juan Basin, New Mexico and Colorado: New Mexico Bureau of Mines and Mineral Resources Bulletin 146, Socorro, p. 13–40 (published in cooperation with the Texas Bureau of Economic Geology Report of Investigations 218, Austin, and the Colorado Geological Survey, Division of Minerals and Geology, Department of Natural Resources Resource Series 31, Golden).

Barwis, J. H., 1976, Internal geometry of Kiawah Island beach ridges, *in* M. O. Hayes, and T. W. Kana, eds., Terrigenous clastic depositional environments: University of South Carolina Coastal Research Division Technical Report 11–CRD, Columbia, p. II–115 to II–125.

Benton, M. J., and D. A. T. Harper, 1997, Basic paleontology: Addison Wesley Longman, Harlow, England, 342 p.

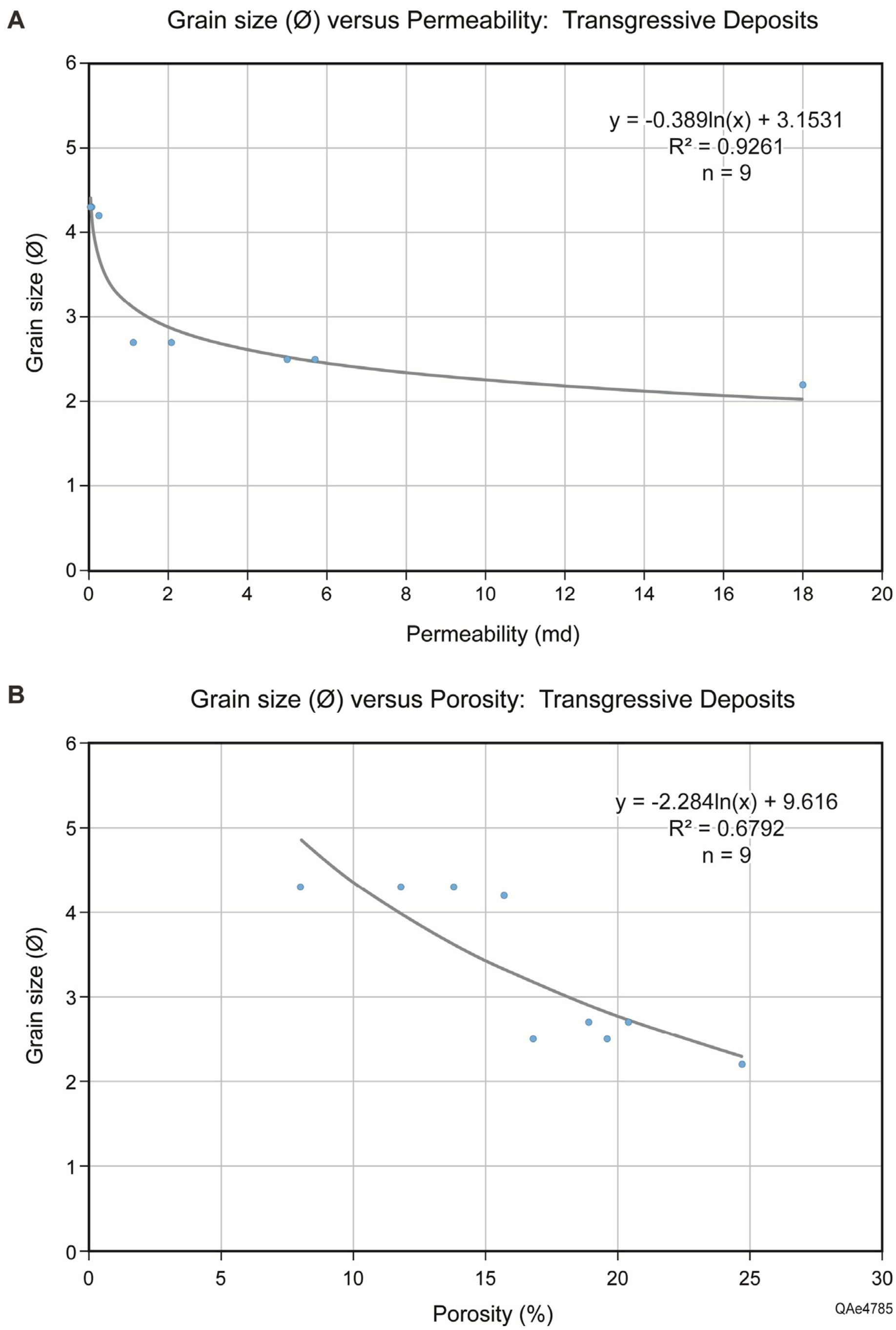

Figure 18. Grain size (ϕ units) versus reservoir-quality data for transgressive deposits. (A) Permeability and (B) Porosity.

Bernard, H. A., R. J. LeBlanc, and C. F. Major, Jr., 1962, Recent and Pleistocene geology of Southeast Texas, *in* E. H. Rainwater and R. P. Zingula, eds., Geology of the Gulf Coast and Central Texas and guidebook of excursions: Houston Geological Society, p. 175–225.

Bhattacharya, J. P., and J. A. MacEachern, 2009, Hyperpycnal rivers and prodeltaic shelves in the Cretaceous seaway of North America: Journal of Sedimentary Research, 2009, v. 79, p. 184–209.

Blakey, R., 2014, Paleogene-Eocene paleogeography of North America: Paleogeography and geologic evolution of North America, <http://www2.nau.edu/rcb7/namPe50.jpg> Last Accessed June 13, 2016.

Bromley, R. G., and U. Asgaard, 1991, Ichnofacies: A mixture of taphofacies and biofacies: *Lethaia*, v. 24, p. 153–163.

Condon, S. M., E. A. Johnson, R. C. Milici, and J. E. Fassett, 1997, Geologic mapping and fracture studies of the Upper Cretaceous Pictured Cliffs Sandstone and Fruitland Formation in selected parts of La Plata County, Colorado: U.S. Geological Survey, Open-File Report 97–59, variously paginated.

Cumella, S. P., 1981, Sedimentary history and digenesis of the Pictured Cliffs Sandstone, San Juan Basin, New Mexico and Colorado: University of Texas at Austin, Texas Petroleum Research Committee Report UT 81–1, 219 p.

Cumella, S. P., 1983, Relation of Upper Cretaceous regressive sandstone units of the San Juan Basin to source area tectonics, *in* M. W. Reynolds and E. D. Dolly, eds., Mesozoic paleogeography of west-central United States: Society of Economic Paleontologists and Mineralogists, Rocky Mountain Section, p. 189–199.

Curray, J. R., F. J. Emmel, and P. J. S. Crampton, 1969, Holocene history of a strand plain, lagoonal coast, Nayarit, Mexico, *in* A. A. Castanares and F. B. Phleger, eds., Coastal lagoons:

A symposium: *Universidad Nacional Autonoma*, Mexico City, p. 63–100.

Dalrymple, R. W., and K. Choi, 2007, Morphologic and facies trends through the fluvial–marine transition in tide-dominated depositional systems: A schematic framework for environmental and sequence-stratigraphic interpretation: Earth-Science Reviews, v. 81, p. 135–174.

Davies, D. K., F. G. Ethridge, and R. R. Berg, 1971, Recognition of barrier environments: American Association of Petroleum Geologists Bulletin, v. 55, p. 550–565.

Davies, J. L., 1964, A morphogenic approach to world shorelines: *Zeitschrift für Geomorphologie*, v. 8, p. 27–42.

Debus, R. W., 1996, Bob West and Lopeno fields: Structure and stratigraphy of two significant Upper Wilcox fields in South Texas: Gulf Coast Association of Geological Societies Transactions, v. 46, p. 87–107.

de Mowbray, T., and M. J. Visser, 1984, Reactivation surfaces in subtidal channel deposits, *Oosterschelde*, southwest Netherlands: Journal of Sedimentary Petrology, v. 54, p. 811–824.

Dickinson, K. A., 1971, Grain size distribution and the depositional history of northern Padre Island, Texas: U.S. Geological Survey Professional Paper 750C, p. C1–C6.

Dominguez, J. M. L., L. Martin, and A. C. S. P. Bittencourt, 1987, Sea-level history and Quaternary evolution of river mouth-associated beach-ridge plains along the east-southeast Brazilian coast, *in* D. Nummedal, O. H. Pilkey, and J. D. Howard, eds., Sea-level fluctuations and coastal evolution: Society of Economic Paleontologists and Mineralogists Special Publication 41, Tulsa, Oklahoma, p. 115–127.

Dott, R. H., Jr., and J. Bourgeois, 1982, Hummocky stratification: Significance of its variable bedding sequences: Geologic Society of America Bulletin, v. 93, p. 633–680.

Dutton, S. P., 1987, Diagenesis and burial history of the Lower Cretaceous Travis Peak Formation East Texas: Texas Bureau of Economic Geology Report of Investigations 164, Austin, 58 p.

Dutton, S. P., and R. G. Loucks, 2010, Diagenetic controls on evolution of porosity and permeability in lower Tertiary Wilcox sandstones from shallow to ultradeep (200–6700 m) burial, Gulf of Mexico Basin, U.S.A.: Marine and Petroleum Geology, v. 27, p. 69–81.

Dutton, S. P., W. A. Ambrose, and R. G. Loucks, 2016, Diagenetic controls on reservoir quality in deep upper Wilcox sandstones in the Rio Grande Delta system, South Texas: Gulf Coast Association of Geological Societies Journal, v. 5, p. 95–110.

Erpenbeck, M. F., 1979, Stratigraphic relationships and depositional environments of the Upper Cretaceous Pictured Cliffs Sandstone and Fruitland Formation, southwestern San Juan Basin, New Mexico: M.S. Thesis, Texas Tech University, Lubbock, Texas, 78 p.

Fassett, J. E., 2000, Geology and coal resources if the upper Cretaceous Fruitland Formation, San Juan Basin, New Mexico and Colorado, *in* M. A. Kirschbaum, L. N. R. Roberts, and L. R. H. Biewick, eds., Geologic assessment of coal in the Colorado Plateau: Arizona, Colorado, New Mexico, and Utah: U.S. Geological Survey Professional Paper 1625–B, Chapter Q, 60 p.

Fassett, J. E., and J. S. Hinds, 1971, Geology and fuel resources of the Fruitland Formation and Kirtland Shale of the San Juan Basin, New Mexico and Colorado: U.S. Geological Survey, Professional Paper 676, 76 p.

Flores, R. M., and M. F. Erpenbeck, 1981, Differentiation of delta front and barrier lithofacies of the Upper Cretaceous Pictured Cliffs Sandstone, southwestern San Juan Basin, New Mexico: The Mountain Geologist, v. 18, no. 2, p. 23–34.

Frey, R. W., S. G. Pemberton, and T. D. A. Saunders, 1990, Ichnofacies and bathymetry: A passive relationship: Journal of Paleontology, v. 64, p. 155–158.

Galloway, W. E., and E. S. Cheng, 1985, Reservoir facies architecture in a microtidal barrier system: Frio Formation, Texas Gulf Coast: Texas Bureau of Economic Geology Report of Investigations 144, Austin, 36 p.

Galloway, W. E., 1986, Reservoir facies architecture of microtidal barrier systems: American Association of Petroleum Geologists Bulletin, v. 70, p. 787–808.

Galloway, W. E., P. E. Ganey-Curry, X. Li, and R. T. Buffler, 2000, Cenozoic depositional history of the Gulf of Mexico Basin: American Association of Petroleum Geologists Bulletin, v. 84, p. 1743–1774.

Galloway, W. E., T. L. Whiteaker, and P. E. Ganey-Curry, 2011, History of Cenozoic North American drainage basin evolution, sediment yield, and accumulation in the Gulf of Mexico Basin: Geosphere, v. 7, p. 938–973.

Gani, M. R., J. P. Bhattacharya, and J. A. MacEachern, 2008, Using ichnology to determine the relative influence of waves, storms, tides, and rivers in deltaic deposits: Examples from Cretaceous Western Interior seaway, U.S.A., *in* J. MacEachern, K. L. Bann, M. K., Gingras, and S. G. Pemberton, eds., Applied ichnology: Society of Economic Paleontologists and Mineralogists Short Course Notes 52, Tulsa, Oklahoma, p. 209–225.

Hargis, R. N., 1985, Proposed lithostratigraphic classification of the Wilcox Group of South Texas: Gulf Coast Association of Geological Societies Transactions, v. 35, p. 107–116.

Hayes, M. O., 1976, Morphology of sand accumulation in estuaries: an introduction to the symposium, *in* L. E. Cronin, ed., Estuarine Research, v. II: Geology and engineering: Academic Press, New York, p. 3–22.

Hayes, M. O., 1979, Barrier island morphology as a function of tidal and wave regime, *in* S. P. Leatherman, ed., Barrier islands from the Gulf of St. Lawrence to the Gulf of Mexico: Academic Press, New York, New York, p. 1–28.

Hill, E. W., and R. E. Hunter, 1976, Interaction of biological and geological processes in the beach and nearshore, northern Padre Island, Texas, *in* Davis, R. A., Jr. and Ethington, R. L., eds., Beach and nearshore sedimentation: Society of Economic Paleontologists and Mineralogists Special Publication 24, Tulsa, Oklahoma, p. 169–187.

Hodge, J. A., 1981, Erosion of the North Santee River Delta and development of a flood-tidal complex: M.S. Thesis, University of South Carolina, Columbia, 151 p.

Howard, J. D., and Reineck, H. E., 1972, Physical and biogenic sedimentary structures of the nearshore shelf: *Senckenberg Maritima*, v. 4, p. 81–123.

Hoyt, J. H., 1969, Chenier versus barrier: Genetic and stratigraphic distinction: American Association of Petroleum Geologists Bulletin, v. 53, p. 299–306.

Hoyt, J. H., and V. J. Henry, 1967, Influence of island migration on barrier island sedimentation: Geological Society of America Bulletin, v. 78, p. 1125–1136.

Joyce, J. G., 1954, Stratigraphy of the Wilcox sands of Zapata County, Texas: Gulf Coast Association of Geological Societies Transactions, v. 4, p. 11–18.

Kraft, J. C., and C. J. John, 1979, Lateral and vertical facies relations of transgressive barrier: American Association of Petroleum Geologists Bulletin, v. 63, p. 2145–2163.

Kumar, N., and J. E. Sanders, 1976, Inlet sequence: A vertical succession of sedimentary structures and textures created by the lateral migration of tidal inlets: Sedimentology, v. 21, p. 491–532.

Kvale, E. P., A. W. Archer, and H. R. Johnson, 1989, Daily, monthly and yearly tidal cycles within laminated siltstones of the Mansfield Formation (Pennsylvanian) of Indiana: Geology, v. 17, p. 365–368.

Kvale, E. P., and A. W. Archer, 1990, Tidal deposits associated with low-sulfur coals, Brazil Fm. (Lower Pennsylvanian), Indiana: Journal of Sedimentary Petrology, v. 60, p. 563–574.

Levin, D. M., 1983, Deep Wilcox structure and stratigraphy in the Fandango Field area, Zapata County, Texas: Gulf Coast Association of Geological Societies Transactions, v. 33, p. 131–138.

Loucks, R. G., M. M. Dodge, and W. E. Galloway, 1984, Regional controls on diagenesis and reservoir quality in lower Tertiary sandstones along the Texas Gulf Coast, *in* D. A. MacDonald and R. C. Surdam, eds., Clastic diagenesis: American Association of Petroleum Geologists Memoir 37, Tulsa, Oklahoma, p. 15–45.

Loucks, R. G., M. M. Dodge, and W. E. Galloway, 1986, Controls on porosity and permeability of hydrocarbon reservoirs in lower Tertiary sandstones along the Texas Gulf Coast: Texas Bureau of Economic Geology Report of Investigations 149, Austin, 78 p.

MacEachern, J., K. Bann, J. P. Bhattacharya, and C. D. Howell, 2005, Ichnology of deltas; organism responses to the dynamic interplay of rivers, waves, storms and tides, *in* L. Giosan and J. P. Bhattacharya, eds., River deltas: Concepts, models and examples, SEPM Special Publication, v. 83, p. 49–85.

Manfrino, C., 1984, Stratigraphy and palynology of the upper Lewis Shale, Pictured Cliffs Sandstone, and lower Fruitland Formation (Upper Cretaceous) near Durango, Colorado: The Mountain Geologist, v. 21, no. 4, p. 115–132.

Meyerhoff, J. C., and R. Braddock, 1998, Loma Vieja Field: structural geology and related velocity fault shadow in the Upper Wilcox (Fandango) in South Texas: Gulf Coast Association of Geological Societies Transactions, v. 48, p. 235–252.

Mulder, T., J. P. M. Syvitski, S. Migeon, J.-C. Faugères, and B. Savoye, 2003, Marine hyperpycnal flows: Initiation, behavior and related deposits. A review: Marine and Petroleum Geology, v. 20, p. 861–882.

Myrow, P. M., and J. B. Southard, 1996, Tempestite deposition: Journal of Sedimentary Research, v. 66, p. 875–887.

Neill, C. A., and M. A. Allison, 2005, Subaqueous deltaic formation on the Atchafalaya Shelf, Louisiana: Marine Geology, v. 214, p. 411–430.

Petter, A. L., and R. J. Steel, Hyperpycnal flow variability and slope organization on an Eocene shelf margin, Central Basin, Spitsbergen: American Association of Petroleum Geologists Bulletin, v. 90, p. 1451–1472.

Pilkey, O. H., and T. W. Davis, 1987, An analysis of coastal recession models: North Carolina coast, *in* D. Nummedal, O. H. Pilkey, and J. D. Howard, eds., Sea-level fluctuations and coastal evolution: Society of Economic Paleontologists and Mineralogists Special Publication 41, Tulsa, Oklahoma, p. 59–68.

Reineck, H. E. and F. Wunderlich, 1968, Classification and origin of flaser and lenticular bedding: Sedimentology, v. 11, p. 99–104.

Reinson, G. E., 1984, Barrier-island and associated strand-plain systems, *in* R. G. Walker, ed., Facies models: Geological Association of Canada Geoscience Canada Reprint Series 1, St. John's, Newfoundland, p. 119–140.

Robinson, B. M., S. A. Holditch, and W. J. Lee, 1986, A case study of the Wilcox (Lobo) trend in Webb and Zapata counties, TX: Journal of Petroleum Technology, v. 38, p. 1355–1364.

Rolf, E. G., 1987, Structural framework and sand genesis of the Wilcox Group, Travis Ward Field, Jim Hogg County, Texas: Gulf Coast Association of Geological Societies Transactions, v. 37, p. 207–216.

Ruby, C. H., 1981, Clastic facies and stratigraphy of a rapidly retreating cuspate foreland, Cape Romain, South Carolina: Ph.D. Dissertation, University of South Carolina, Columbia, 207 p.

Seilacher, A., 1964, Biogenic sedimentary structures, *in* J. Imbrie and N. Newell, eds., Approaches to paleoecology: John Wiley and Sons, New York, New York, p. 296–316.

Stephens, D. G., D. S. Van Nieuwenhuise, P. Mullin, C. Lee, and W. H. Kanes, 1976, Destructive phase of deltaic development: North Santee River Delta: Journal of Sedimentary Petrology, v. 46, p. 132–144.

Stricklin, F. L., 1994, Genetic variations in a growth-fault system: Gulf Coast Association of Geological Societies Transactions, v. 44, p. 717–723.

Swift, D. J. P., 1968, Coastal erosion and transgressive stratigraphy: Journal of Geology, v. 76, p. 444–456.

Taylor, T. R., M. R. Giles, L. A. Hathon, T. N. Diggs, N. R. Braunsdorf, G. V. Birbiglia, M. G. Kittridge, C. I. Macaulay, and I. S. Espejo, 2010, Sandstone diagenesis and reservoir quality prediction: Models, myths, and reality: American Association of Petroleum Geologists Bulletin, v. 94, p. 1093–1132.

Tokar, F. J., Jr., and J. E. Evans, 1993, Depositional environments of the Pictured Cliffs Sandstone, Late Cretaceous, near Durango, Colorado: Ohio Journal of Science, v. 93, v. 4, p. 83–89.

Tyler, N., and W. A. Ambrose, 1986, Depositional systems and oil and gas plays in the Cretaceous Olmos Formation, South Texas: Texas Bureau of Economic Geology Report of Investigations 152, Austin, 42 p. plus plate.

Walker, R. G., and A. G. Plint, 1992, Wave- and storm-dominated shallow marine systems, *in* R. G. Walker, ed., Facies models: Geological Association of Canada Geoscience Canada Reprint Series 1, St. John's, Newfoundland, p. 219–238.

White, C. D., B. J. Willis, S. P. Dutton, J. P. Bhattacharya, and K. Narayanan, 2004, Sedimentology, statistics, and flow behavior for a tide-influenced deltaic sandstone, Frontier Formation, Wyoming, United States, *in* G. M. Grammer, P. M. Harris, and G. P. Eberli, eds., Integration of outcrop and modern analogs in reservoir modeling: American Association of Petroleum Geologists Memoir 80, Tulsa, Oklahoma, p. 129–152.

Wilkinson, B. H., and R. A. Basse, 1978, Late Holocene history of the central Texas coast from Galveston Island to Pass Cavallo: Geological Society of America Bulletin, v. 89, p. 1592–1600.